High-precision atmospheric oxygen measurement comparisons between a newly built CRDS analyzer and existing measurement techniques

Tesfaye A. Berhanu[1,2], John Hoffnagle[2], Chris Rella[2], David Kimhak[2], Peter Nyfeler[1], Markus Leuenberger[1]

[1]*Climate and Environmental Physics, Physics Institute and Oeschger Centre for Climate Change Research, University of Bern, Bern, Switzerland*

[2]*Picarro Inc., 3105 Patrick Henry Drive, Santa Clara, CA, USA*

Abstract

Carbon dioxide and oxygen are tightly coupled in land-biospheres CO_2 - O_2 exchange processes, while they are not coupled in oceanic exchange. For this reason, atmospheric oxygen measurements can be used to constrain the global carbon cycle, especially oceanic uptake. However, accurately quantifying the small (~1-100 ppm) variations in O_2 is analytically challenging due to the very large atmospheric background which constitutes about 20.9 % (~209500 ppm) of atmospheric air. Here we present detailed description of the analyzer and its operating principles as well as comprehensive laboratory and field studies for a newly developed high-precision oxygen mixing ratio and isotopic composition analyzer (Picarro G-2207) that is based on cavity ring-down spectroscopy (CRDS). From the laboratory tests, we have calculated a short-term precision (standard error of one-minute O_2 mixing ratio measurements) of < 1 ppm for this analyzer based on measurements of eight standard gases analyzed for two hours consecutively. In contrast to the currently existing techniques, the instrument has an excellent long-term stability and therefore a calibration every 12 hours is sufficient to get an overall uncertainty of < 5 ppm. Measurements of

Formatted: Subscript

ambient air were also conducted at the High-Altitude Research Station, Jungfraujoch and the Beromünster tall tower in Switzerland. At both sites, we observed opposing and diurnally varying CO_2 and O_2 profiles due to different processes such as combustion, photosynthesis and respiration. Based on the combined measurements at Beromünster tower, we determined height dependent O_2:CO_2 oxidation ratios varying between -0.98 to -1.60 , which increase with the height of the tower inlet, possibly due to different source contribution such as natural gas combustion with high oxidation ratio and biological processes which are at the lower end.

1. Introduction

Atmospheric oxygen comprises about 20.9 % of the global atmosphere and in the past decade its concentration decreased at a rate of ~ 20 per meg yr^{-1} (Keeling and Manning, 2014) mainly associated with the increase in fossil fuel combustion. Note that the variations in atmospheric O_2 is expressed in units of per meg due to its small variations with respect to a large background and to account for dilution effects from CO_2 or any other gas of relevant amount change which is expressed as:

~~$$\left(\frac{O_2}{N_2}\right)(per\ meg) = \left(\frac{\left(\frac{O_2}{N_2}\right)_{reference}}{\left(\frac{O_2}{N_2}\right)_{sample}} - 1\right).10^6$$~~

$$\delta\left(\frac{O_2}{N_2}\right)(per\ meg) = \left(\frac{\left(\frac{O_2}{N_2}\right)_{sample}}{\left(\frac{O_2}{N_2}\right)_{reference}} - 1\right).10^6 \quad (1)$$

In contrast, the global average atmospheric CO_2 mixing ratio increased to ~~402~~405.~~8~~ 0 ppm averaged over ~~2016~~ 2017 ~~(predicted to grow by 2 % in 2017)~~ since its preindustrial value of 280 ppm (Le Quéré et al., 2017). As the variability of atmospheric oxygen is directly linked to the carbon cycle, both its short and long-term observations can be used to better constrain the carbon cycle. For example, since first suggested by Keeling and Shertz (1992) the long-term trends derived from concurrent measurements of atmospheric CO_2 and O_2 have been

Formatted: Subscript

Formatted: Font: Times New Roman, Not Italic

Formatted: Highlight

Formatted: Highlight

widely used to quantify the partitioning of atmospheric CO_2 between the land-biosphere and oceanic sinks (Battle et al., 2000; Goto et al., 2017; Manning and Keeling, 2006; Valentino et al., 2008). This method hinges on the linear coupling between CO_2 and O_2 with an oxidation ratio (OR defined as the stoichiometric ratio of exchange during various process such as photosynthesis and respiration) of 1.1 for the terrestrial biosphere photosynthesis-respiration processes (α_b) and 1.4 for fossil fuel combustion (α_f) while they are decoupled for oceanic processes. Meanwhile, the short-term variability in atmospheric oxygen can be used to estimate marine biological productivity and air-sea gas exchange (Keeling et al., 1998; Nevison et al., 2012). However, the accuracy of these estimates is primarily linked to the accuracy and precision of atmospheric O_2 measurements and the assumed ORs for the different processes which are highly variable in contrast to atmospheric CO_2 that can be well measured within the precision guidelines set by the Global Atmospheric Watch (GAW) (± 0.1 ppm for the northern hemisphere).

Currently there are several techniques mostly custom built that can measure atmospheric O_2 variations as oxygen concentration based on interferometric, paramagnetic, UV absorption and fuel cell technology (Keeling, 1988a; Manning et al., 1999; Stephens et al., 2007) or as O_2/N_2 ratios to account for the large background effect using gGas chromatography with thermal conductivity detector (GC-TCD) or ~~Gas~~ gas chromatography coupled to mass spectrometry (GC-MS) (Bender et al., 1994; Tohjima, 2000). Despite the fact that these techniques have been ~~commercially available~~ used for more than two decades, accurate quantification of atmospheric oxygen variability remains challenging primarily because the small ppm-level atmospheric oxygen signal rides on a ~ 210,000 ppm background, which places stringent requirements on the precision and drift of the analysis methods especially for continuous monitoring. (Note that the GAW recommendation for the

measurement precision of O_2/N_2 is 2 per meg). The techniques listed above struggle to routinely achieve the necessary performance for various reasons, including i) instability over time that requires frequent measurement interruption for calibration, ii) measurement bias with ambient and sample temperature and/or pressure, and/or iii) systematic errors in the measurement due to other atmospheric species. Further, some techniques require the use of consumables and rely on high vacuum, which complicates field deployment.

In this manuscript we describe a new high precision oxygen concentration and isotopic composition analyzer by Picarro Inc., Santa Clara, USA (G-2207) based on CRDS technology. Here, we will introduce the analyzer design principles in details, describe the unique features of the analyzer and evaluate its performance based on various independent laboratory and field tests by comparing it with currently existing techniques. Then, we will present and interpret our observations based on field measurements. Finally, we will conclude its overall performance and provide recommendations and possible improvements.

2. Analyzer design principles

The analyzer described here is derived from the Picarro G2000 series of CRDS analyzers. The basic elements have been described elsewhere (Crosson, 2008; Martin et al., 2016; Steig et al., 2014): briefly, the instrument is built around a high-finesse, traveling-wave optical cavity, which is coupled to either of two single-frequency Distributed ~~FB~~Feedback-stabilized semiconductor lasers. One cavity mirror is mounted on a piezoelectric translator (PZT) to allow fine tuning of the cavity resonance frequencies. A semiconductor optical amplifier between the laser sources and the cavity boosts the laser power and serves as a fast-optical switch. The cavity body is constructed of invar and enclosed in a temperature stabilized box (T = 45° C, stabilized to approximately 0.01 °C) for dimensional and spectroscopic stability. A vacuum pump pulls the gas to be sampled through the cavity and a

proportional valve between the cavity and the pump maintains the sample pressure in the cavity at a value of 340 hPa, with variations on the order of 1 Pa. The instrument has a wavelength monitor, based upon measurements of interference fringes from a solid etalon, which is used to control the laser wavelength by adjusting the laser temperature and current. A high-speed photodiode monitors the optical power emerging from the cavity. The instrument's data acquisition system sweeps the laser frequency over the spectral feature to be measured, modulates the laser output to initiate ring-downs, and fits the ring-down signal to an exponential function to generate a spectrogram of optical loss versus laser frequency. For this instrument the empty cavity ring-down time constant is about 39 μs. Subsequent program modules compare the measured loss spectrum to a spectral model, using non-linear least-squares fitting (Press et al., 1986) to find the best-fit model parameters and thereby obtain a quantitative measure of the absorption due to the target molecule, and finally apply a calibration factor to the optical absorption to deduce the molecular concentration. When operating in its normal gas analysis mode, the instrument acquires about 200-300 ring-downs per second and achieves a noise equivalent absorption of typically about 10^{-11} cm^{-1} $Hz^{-1/2}$, with some variation between instruments.

Formatted: English (United States)

Formatted: English (United States)

The primary goal when designing this analyzer was to measure the molecular oxygen concentration with few-per-meg level precision and stability. In this context operational stability is as important as signal-to-noise. Our experience has been that the most stable operation of the analyzer is achieved when the optical phase length of the cavity is held as nearly constant as possible. In this case the free spectral range (FSR, 0.0206 cm^{-1}) of the temperature stabilized, invar ring-down cavity provides a better optical frequency standard than the etalon-based wavelength monitor, which in turn allows more consistent measurements of absorption line width and integrated absorption line intensity (Steig et al.,

Formatted: English (United States)

2014). For a small, field-deployable instrument, it is not practical to stabilize the absolute frequencies of the cavity modes to an optical frequency standard (Hodges et al., 2004) but the oxygen lines themselves, under conditions of constant temperature and pressure, provide an adequate frequency reference. The oxygen spectrum was also used to calibrate the FSR, by comparing a wide (approximately 10 cm^{-1}) FSR-spaced spectrum with the Hitran database (Rothman et al., 2013).

To determine molecular oxygen concentration, the analyzer measures absorption of the Q13Q13 component of the $a^1\Delta_g \leftarrow X^3\Sigma^-_g$ band, at a frequency of 7878.805547 cm^{-1}, according to the latest edition of Hitran (Gordon et al., 2017). This is one of the strongest near-infrared lines of oxygen, well separated from other oxygen lines, and reasonably free of spectral interference from water, carbon dioxide, methane, and other constituents of clean air. The spectral model for this line was developed using reference spectra of clean, dry, synthetic air that were acquired with the same hardware as in the field-deployable analyzer, but with special-purpose software that allows it to operate as a more general spectrometer.

Recently, considerable work has been done to advance the understanding of spectral line shapes and to define functional representations that better describe the processes that determine spectral line shapes than does the Voigt model (Hartmann et al., 2008; Tennyson et al., 2014, Tran et al., 2019). Line shape studies have been published for the 1.27 μm band of O_2 (Fleisher et al., 2015; Lamouroux et al., 2014), though not to our knowledge for the Q branch. The apparatus used here is not capable of spectroscopic studies of comparable precision; the absolute temperature and pressure monitoring and especially the frequency metrology are far too crude for that purpose. Our goal is merely to define a simple model of the Q13Q13 line that is adequate for least-squares retrievals of the O_2 absorption under the limited range of conditions (stabilized temperature and pressure) that the operational analyzer

experiences in the field. The CRDS analyzers use the Galatry function (Varghese and Hanson, 1984), which is distinctly better than the Voigt and still easily and quickly evaluated for line shape modeling. Ultimately, the usefulness of the spectral model is to be evaluated by the precision and stability of the O_2 measurements when compared with established techniques. ~~We also note at this point that Sironneau, Fleisher, and Hodges have made detailed measurements of lines in the R branch of the $a^1\Delta_g \leftarrow X^3\Sigma^-_g$ band and observed departures from simple, linear absorption, which they interpret as arising from collision-induced absorption (Fleisher et al., 2015). This has two important consequences for O_2 monitoring: the line strength is not independent of sample pressure, and optical absorption is not linear in laser intensity. We do not expect these effects to be too severe for our application because the ring-down cavity is stabilized to a very narrow range of temperature and pressure. In addition, the optical power in the ringdown cavity set by the ring-down detector threshold, which is used to trigger the laser shutoff and subsequent ring-down waveform acquisition. The fact that all ring-downs occur at the same intracavity power should minimize the effect of collision-induced absorption. We have observed some excess noise on the ring-down time constants for the highest loss points at the peak of the Q13Q13 line, which might have to do with the fitting of the ring-down signal if absorption is not linear, but we cannot be certain of this explanation at present.~~ Ultimately, the usefulness of the spectral model is to be evaluated by the precision and stability of the O_2 measurements when compared with established techniques.

For spectral model development, this spectrometer has the drawback that the cavity FSR~~, equal to about 0.0206 cm^{-1}~~, is too large to reveal much detail of the absorption line shape, even with the simplifying assumption of a Galatry line shape. We therefore acquired a set of four interleaved spectra, with the PZT-actuated mirror moved to offset the cavity modes of the individual FSR-spaced spectra by one-fourth of an FSR. The precise offsets were

Formatted: English (United States)

determined from fits to the strong and well-isolated O_2 lines in the spectra. From the consistency of the fitted line centers, we estimate that the positioning of the interleaved spectra was accurate to approximately 10 MHz. The spectrum of the Q13Q13 line acquired in this manner is shown in Figure 1, together with the best-fit Galatry function. It stands out that the residuals ~~that~~ are largely ~~an odd function of~~odd in detuning from the line center: this shows the limitations of the Galatry model in this case, since the Galatry function is purely even about the line center. The shape of the absorption line in this model is specified by two dimensionless parameters: the collisional broadening parameter

$$y = \gamma / \sigma_D \quad (1\text{~~1~~}2)$$

and the collisional narrowing parameter

$$z = \beta / \sigma_D \quad (2\text{~~2~~}3)$$

where γ is the frequency of broadening transitions, β is the ~~frequency of narrowing collisions~~velocity change collision rate, and σ_D is the 1/e Doppler half-width~~Doppler width~~ of the transition, given by

$$\sigma_D = \nu_0(2k_BT/Mc^2)^{1/2} \quad (3\text{~~3~~}4)$$

where ν_0 is the transition frequency, k_B is Boltzmann's constant (J. K^{-1}), T is the sample temperature (K), M is the molecular mass (amu), and c is the speed of light (m/s). Figure 2 shows the values of y and z obtained from spectra acquired in the same way as Figure 1, as a function of cavity pressure. The values depend linearly on pressure, as expected from the Galatry model, but the unconstrained linear fits do not go precisely through the origin. It is not clear whether this represents a breakdown of the Galatry model or simply reflects the limited quality of the data set. The slope of y can be converted to an air-broadened collisional width γ_{air} = 0.0442 cm^{-1}/atm, which agrees with the Hitran value of 0.0460 cm^{-1}/atm (~~Rothman et al., 2013~~) (Gordon et al., 2016) to within the uncertainty estimate stated by

Formatted: Superscript

Field Code Changed

Hitran (uncertainty code 4 for γ_{air} corresponding to 10% --20% relative uncertainty). The slope of z can be interpreted in terms of the optical diffusion coefficient (Fleisher et al., 2015), yielding D = 0.285 cm^2 s^{-1}, compared to the literature value of 0.233 cm^2 s^{-1} for O_2 in air at 45 °C (Marrero and Mason, 1972). Although the anticipated use of the analyzer is for ambient air samples having a very small range of O_2 concentrations, we did investigate the variation of the line shape in binary mixtures of O_2 and N_2 shown in Figure 3. The error bars are taken from the output of the Levenberg-Marquardt fitting routine (Press et al., 1992). The dependence of the collisional broadening parameter z on O_2 mole fraction was considered too small to be significant, but the variation in y was used in the subsequent analysis of the air samples. Note that Wójtewicz et al. (Wójtewicz et al., 2014) also found collisional broadening coefficients for nitrogen to be slightly larger than for oxygen in measurements of one O_2 line in the B-band.

The primary goal in designing the analyzer was to achieve high enough precision to make meaningful measurements of O_2 in clean atmospheric samples. Although the current best practice for such high-precision measurements is to work with dried samples, we decided to include high precision measurements of water vapor. There were two reasons for this decision: one is to serve as a monitor for residual water vapor, which is difficult to remove completely from the ring-down cavity and associated sample handling hardware, and the second and more ambitious reason was to see how well the effect of water vapor could be corrected for ~~in~~ measurements of undried ambient air. While it was considered unlikely that measurements of undried air could compete in accuracy with those of dried air, it might be possible to correct for water vapor well enough to enable useful measurements in some circumstances without the expense and inconvenience of drying the sample. For this purpose, a second laser was added, which probes the $7_{1,6} \rightarrow 8_{4,5}$ component of the $2v_3$ band of water

Formatted: English (United States)

Formatted: English (United States)

vapor, at a frequency of 7816.75210 cm^{-1} (Gordon et al., 2017). The Galatry model was used to fit spectra of synthetic air humidified to various levels of water vapor concentration. These fits also included two other nearby, very weak water lines, with intensities less than 1% of the strong transition, in order that their absorption should not perturb the line shape of the main transition. Results for the shape of the 7816.75210 cm^{-1} line are shown in Figure 4. At the level that we can measure, only the y-parameter has a meaningful variation with water concentration. From the linear fit one obtains a pressure broadening coefficient for air, γ_{air} = 0.0752 cm^{-1}/atm, in reasonable agreement with the Hitran value γ_{air} = 0.0787 cm^{-1}/atm (Gordon et al., 2017), and a self-broadening coefficient γ_{self} = 0.413 cm^{-1}/atm, to be compared with the Hitran value γ_{self} = 0.366 cm^{-1}/atm. Since the uncertainty estimate for the Hitran values is 10 % to 20 %, this level of agreement seems reasonable.

We also looked at absorption from water near the Q13Q13 absorption line of O_2. These spectra were measured in a background of pure nitrogen to reveal the very weak lines interfering with the O_2 measurement. Without the strong O_2 lines, it was impossible to interleave FSR-spaced spectra, so in this case the frequency axis comes from the analyzer's wavelength monitor. The upper panel of Figure 5 shows the spectrum of saturated water vapor in nitrogen, together with a fit to a Voigt model of the molecular lines. The measurement was made at a pressure of 340 hPa and temperature of 45° C. ~~The two most prominent features in this spectrum are actually the Q17R16 and Q13Q13 lines from traces of O_2 remaining in the sample while the other features are from water.~~ The main features are the Q13Q13 line from trace contamination of oxygen in the sample and several lines that arise from normal water ($^1H_2{}^{16}O$, AFGL abbreviation 161) and deuterated water ($^1H^2H^{16}O$, AFGL abbreviation 162, also abbreviated HDO). The lower panel of Figure 5 shows the lines tabulated in Hitran. Immediately after the data in Figure 5 were acquired, measurements were also made at 7816.85210 cm^{-1}, to establish the

Formatted: English (United States)

relationship between the absorption strengths in the two spectral regions. ~~All the water lines that were observed, in both spectral regions, are from the dominant 161 isotopolgue of water, so changes in isotopic composition of atmospheric water does not lead to variation in the relative strengths of the lines we measure.~~ The relative intensities of the 161 and 162 lines change with variations in the isotopic composition of the water, but fortunately the direct interference with the oxygen Q13Q13 lines comes entirely from the 161 isotopologue, with the strongest 162 line being separated by approximately 8 line widths (FWHM) from the Q13Q13 line. Hitran simulations for molecules other than water that are expected to be present in clean, ambient air indicate that direct interference with the Q13Q13 line should be negligible at the level of precision considered here. In the case of CO_2, the dilution of oxygen due to 400 ppm of CO_2 is significant, and larger than any direct spectral interference.

Finally, we investigated the influence of water vapor on the shape of the O_2 Q13Q13 line. Switching between the two lasers sources, we acquired FSR-spaced spectra of humidified synthetic air, alternately covering the 7817 cm^{-1} and 7878 cm^{-1} regions. Individual spectra were acquired in less than 2 s, so changes in water vapor concentration between spectra were small. These spectra, with frequency resolution of 0.0206 cm^{-1}, were analyzed by nonlinear least-squares fitting with the following spectral models: the 7817 cm^{-1} spectra were modeled as the sum of an empty-cavity baseline having an adjustable offset level and slope and three water peaks and the two weak perturbing peaks. The molecular absorption of the main peak was expressed as an adjustable amplitude, A_w, multiplying a dimensionless, area-normalized Galatry function (Varghese and Hanson, 1984). The weak perturbers were modeled by Voigt profiles with amplitudes and line widths that constrained to be in fixed ratios to the strong line, and therefore added no new degrees of freedom to the fitting procedure. Since the amplitude A_w multiplies an area-normalized shape function, it is

Formatted: English (United States)

essentially equivalent to the area of the absorption line, to the extent that the Galatry model provides a valid description of the line shape. The Doppler width of the Galatry function was fixed based on the measured cell temperature, the y-parameter was allowed to vary, and the z-parameter was constrained to be proportional to y, based on measurements summarized in Figure 2~~the earlier measurements~~. In addition, the center frequency of the Galatry function was adjusted to match the data set, giving a total of five free parameters for this fit. The 7878 cm^{-1} spectra were modeled with an adjustable baseline offset and slope and molecular absorption amplitude, A_{O2}, describing the Q13Q13 O_2 line. Here, too, the y-parameter and centration of the O_2 lines were allowed to adjust, and the z-parameter was constrained to be proportional to y. The weak water lines interfering with oxygen absorption were included in the model, but with no additional free parameters, rather the amplitudes were preset based on the measured water absorption at 7817 cm^{-1} and the previously determined amplitude relationships between the water lines. This procedure does not account for variations in HDO abundance, which may introduce some systematic error into the water vapor correction for samples of unusual isotopic composition, but it should accurately model the most important lines that interfere with the oxygen measurement. Collisional broadening of the Q13Q13 O_2 line by water vapor is shown in Figure 6. From the linear fit one obtains a coefficient for collisional broadening of the Q13Q13 line by water vapor of γ_{water} = 0.0442 cm^{-1}/atm. We are not aware of previous measurements of this quantity.

The alternating measurements at 7817 cm^{-1} and 7878 cm^{-1} also calibrated the relationship between water mole fraction and the absorption at 7817 cm^{-1}, using a dilution analysis described by Filges et al. (Filges et al., 2018), who showed that the results obtained this way agree well with water vapor fractions measured with a conventional hygrometer. Figure 7 shows the measured amplitudes of the water and oxygen lines for samples of variable

Formatted: English (United States)

Formatted: English (United States)

287 humidity. Since the air came from a tank of constant composition, the oxygen concentration
288 changes due to dilution of oxygen when water is added. Assuming that this is the sole cause
289 of the change in measured absorption, since the line shapes were being constantly adjusted to
290 account for changes in collisional broadening, it is straightforward to deduce the relation
291 between the water fraction and the absorption amplitude. This calibration was used to
292 generate the water fraction axes in Figures 4 and 6. We note that we did not take particular
293 care to control or measure the quantity of dissolved gases, especially oxygen and carbon
294 dioxide, in the water used for this experiment. While these gases would not significantly
295 affect the water calibration, they may affect the water vapor correction of the oxygen
296 measurement at the ppm level. More work needs to be done to investigate the water vapor
297 correction of the oxygen measurement.

298 The observations described above were used to design a method to measure oxygen
299 concentration in ambient air. Gas from the inlet to the analyzer is drawn through the cavity at
300 a rate of about 100 sccm (standard cubic centimeter per minute) and the conditions in the
301 cavity are held stable at 340 hPa and 45° C. In its analysis mode the analyzer alternately
302 measures ring-downs in the 7817 cm^{-1} and 7878 cm^{-1} regions. At 7878 cm^{-1} measurements are
303 made at 11 different frequencies, spaced by one FSR of the cavity and centered at the peak of
304 the Q13Q13 line. Multiple ring-down measurements are made to improve the precision of the
305 loss determination, with a total of 305 ring-downs allocated to one spectrum. In the 7817 cm^{-1}
306 region measurements are also made at 11 distinct frequencies at FSR spacings. Only 35 ring-
307 downs are allocated to this spectral region, since the measurement of O_2 is much more
308 important than water vapor. The data sets are analysed using a Levenberg-Marquardt fitting
309 routine, which adjusts five free parameters in each region to find the best agreement to a
310 spectral model based on Galatry line shapes, as described above. One of the outputs of the

7878 cm^{-1} fit is the frequency offset of the FSR grid from the center of the Q13Q13 line. This information is used to adjust the position of the PZT actuated mirror to keep the measurements centered on the line, effectively stabilizing the optical path length of the cavity to the frequency of the O_2 line. The reported water fraction is obtained by multiplying the fitted amplitude of the water line by a calibration constant derived from the dilution experiment as explained above. For the O_2 fraction a slightly more complicated procedure is followed. It was observed that the least-squares fitting of the data gives highly correlated results for the amplitude of the absorption line and the line width parameter y. The correlation may be due in part to the fitting procedure itself (Press et al., 1992) and it may also have a contribution from pressure variations that the pressure sensor is unable to detect. The ratio A_{O2}/y can be determined from the fit much more precisely than A_{O2} alone and so gives a more sensitive measurement of molecular absorption. It also has the advantage of being independent of sample pressure, to the extent that the Galatry model applies (Figure 2). However, using the ratio A_{O2}/y as a metric for absorption adds ~~additional~~ more complications if measurements are to be made over a range of O_2 and water concentrations, because the O_2/N_2 ratio and water concentration affect the line width independently of pressure and O_2 concentration alone. To minimize systematic errors due to these broadening effects, we define a nominal y-parameter based on the measured amplitudes of the O_2 and water lines and the line broadening dependences shown in Figures 3 and 4. The measured ratio A_{O2}/y is normalized by the nominal y to obtain a quantity that is ideally independent of pressure and water concentration, and this is the quantity that is multiplied by a calibration constant to give the reported O_2 fraction. In addition, a dry mole fraction is reported for O_2, defined as the directly measured mole fraction corrected for water dilution.

The main goal in developing this instrument was to make high precision measurements of O_2 mole fraction, based on absorption by the dominant $^{16}O_2$ isotopologue. The absorption lines of the rarer isotopologues are also present nearby, so a mode of operation was included in which one laser is scanned over neighboring lines of $^{16}O_2$ and $^{16}O^{18}O$ and the ratio of amplitudes is used to derive an isotopic ratio, reported in the usual delta notation. In this case the operating pressure was reduced to 160 hPa to improve the resolution of the nearby lines. The lines measured were the Q3Q3 line of $^{16}O_2$, at 7882.18670 cm^{-1}, and the Q9Q9 line of $^{16}O^{18}O$, at 7882.050155 cm^{-1}. The measurement procedure is very much like that for the O_2 fraction measurement, so it will not be described in detail, only the main differences will be noted. One is that in determining an isotopic ratio there is no advantage to be obtained from normalizing absorption amplitudes to line widths, instead we simply take the ratio of amplitudes to compute delta. Although the Q9Q9 line and its neighbor Q8Q8 are the strongest ones in this band, absorption by $^{16}O^{18}O$ is still very weak, only about $5x10^{-9}$ cm^{-1} at the line center under the conditions we used. Consequently, the signal-to-noise that can be achieved with this analyzer is not adequate to determine both the amplitude and the width of the $^{16}O^{18}O$ line with useful precision, so in the fitting step the y-parameter of the $^{16}O^{18}O$ line is constrained to be a constant factor times the fitted y-parameter for the $^{16}O_2$ line. Additionally, because of the weakness of the rare isotopologue absorption, the majority of ring-downs in each spectrum is devoted to measuring $^{16}O^{18}O$ i.e. 232 ring-downs in each spectrum versus only 40 for $^{16}O_2$. This implies that the mole fraction measurement in the isotopic mode is much less precise than when the analyzer measures the Q13Q13 line alone.

3. Results and Discussions

3.1. Laboratory tests at Picarro, Santa Clara

3.1.1. Temperature and pressure sensitivity

One set of tests was done to determine how well the goal was met of minimizing the susceptibility of the concentration measurements to uncontrolled noise or drift of the sample temperature and pressure. For these tests the analyzer sampled dry synthetic air from a tank and the temperature and pressure setpoints of the cavity were adjusted upward and downward from the nominal values, to obtain an estimate of the differential response. We express the sensitivity to experimental conditions in relative form, that is the derivative with respect to temperature or pressure divided by the signal under nominal conditions.

From these experiments, we determined a temperature sensitivity of -2.1×10^{-4} K^{-1} and a pressure sensitivity of $+9.8 \times 10^{-6}$ hPa^{-1}. The temperature sensitivity is somewhat larger than expected based on a calculation using Hitran data to estimate the temperature dependences of all the quantities that go into the measured absorption of the Q13Q13 line. The pressure sensitivity is strikingly small, indicating a good cancelation of the pressure dependence of absorption amplitude and line width. Both temperature and pressure sensitivities are small enough to have a negligible effect on short-term precision of measurements made with the stabilized ring-down cavity, though long-term drifts in the sensors are always a matter of concern.

3.1.2. Measurement precision and Drift

Measurement precision was evaluated by analyzing synthetic air containing nominal atmospheric concentrations of CO_2 and CH_4 from an aluminum Luxfer cylinder over a period of several days. The tank, oriented horizontally and thermally insolated (though not controlled), was connected directly to the instrument (S/N TADS2001) with a 2-stage regulator and stainless-steel tubing and reducing the flow with an additional orifice to about 55 sccm. For the isotopic mode of operation, the precision of the measurement was also tested by making repeated measurements from a tank of clean, dry synthetic air.

Figure 8 shows the time series of the precision test data, displaying the reported oxygen concentration, the height of the oxygen absorption peak, the width of the oxygen absorption peak and the ambient temperature. The residual error~~drift~~ of the analyzer, although small, is nevertheless significant given the stringent targets set forth by the WMO-GAW program. Possible sources of ~~drift~~ error include: temperature drifts due to sensor drift or gradients; pressure errors due to sensor drift; optical artifacts such as parasitic reflections, higher order cavity mode excitation, and/or loss nonlinearity that can distort the reported oxygen spectrum. More work is required to identify and eliminate these small drifts.

The Allan standard deviation of the reported O_2 fraction is shown in Figure 9. The ordinate on this plot is the square root of the Allan variance of reported mole fraction, so 1 ppm in these units corresponds to about 5 per meg in the ratio of O_2/ N_2. The precision of averaged measurements improves as $\tau^{-1/2}$ for approximately 5000 s and reaches 1 ppm in less than 10 minutes and remains below 1 ppm for time scales on the order of about 1 hour.

Figure 10 shows the precision of $\delta(^{18}O)$ (uncalibrated) derived from the ratio of lines measured at 7882 cm^{-1}. Because of the weak signal from the $^{16}O^{18}O$ line, it is necessary to average for more than 20 seconds or more to achieve 1‰ precision on the isotopic ratio. As for the concentration measurement, averaging improves the measurement precision for times scale up to about 1 hour.

3.2. Laboratory measurements at the University of Bern

3.2.1. Measurements of standard gases

The performance of the instrument was tested by analyzing eight standard gases with precisely known CO_2 and O_2 compositions (Table 1) using the CRDS analyzer and comparing it to parallel measurements with a paramagnetic oxygen sensor (PM1155 oxygen transducer, Servomex Ltd, UK) embedded to a commercially available Oxzilla fuel cell oxygen analyzer

406 (OXZILLA II, Sable Systems International, USA) (Sturm et al., 2006) as well as with an
407 isotope ratio mass spectrometer (IRMS, Finnigan Delta^{Plus}XP). The design of the
408 measurement set-up is shown in Figure 11. Standard gases were directly connected to the
409 pressure controlling unit, and a multi-port valve (V2) was used to select among the standard
410 gases. The flow from each cylinder was adjusted to about 120 ml min^{-1} which was eventually
411 directed to a selection valve (V1), allowing switching between ambient air and standard gases.
412 Flow towards and out of the Oxzilla was controlled by the pressure controlling unit. The O_2
413 mixing ratio of this incoming gas was first measured on the Paramagnetic O_2 sensor and then
414 directed towards a non-dispersive infrared analyzer (NDIR) (Li-7000, LICOR, USA) for
415 measuring CO_2 and H_2O. The outflow from this analyzer (100 ml min^{-1}) returns to the
416 pressure controlling unit and was eventually divided between the CRDS analyzer (which uses
417 about 75-80 ml min^{-1}) and the IRMS (~ 20 ml min^{-1}) via a Tee-junction. Each cylinder was
418 measured for two hours in each system controlled by a Lab VIEW program.
419 In priori, we investigated the influence of this Tee-junction, which splits the gas flow
420 between the CRDS and the IRMS, on the measured O_2 values. Manning (2001) showed that
421 the fractionation of O_2 in the presence of a Tee-Junction is strongly dependent on the splitting
422 ratios as well as temperature and pressure gradients. Hence, we measured and compared the
423 O_2 mixing ratios of two standard gases (CA07045 and CA060943) in two cases: i) in the
424 presence of a Tee-junction with different CRDS to IRMS splitting ratios and ii) without a
425 Tee-junction so that all gas flow is directed towards the CRDS analyzer. The splitting ratios in
426 these test experiments vary from 1:1 to 1:100, and reversed to change the major flow direction
427 either to the CRDS or the IRMS. Note that the experimental condition in this manuscript is
428 with a 4:1 splitting ratio (i.e. ~ 80 ml min^{-1} towards the CRDS analyzer and ~ 20 ml min^{-1}
429 towards the IRMS).

In the cases of the smaller splitting ratios (1:1, 1:4 and 4:1), which are relevant for the results presented in this study, only minor differences in the measured O_2 mixing ratios were observed when compared to case ~~b~~ ii (i.e. without a Tee-junction). For these two cylinders measured, the average differences in these cases were about 0.5 ppm, calculated as the mean of the differences in the raw O_2 measurements of the last 60 seconds. The negligible fractionation can indeed be the result of smaller splitting ratios while strong influence is usually expected in case of larger splitting ratios (Stephens et al., 2007). For higher splitting ratios, the result seems inconclusive without any dependence on the ratios due to the strong decline in the cylinder temperature (specifically at the pressure gauge) caused by higher flow to achieve the higher splitting ratios (as high as 1:100). Hence, these tests need to be conducted in a temperature controlled condition and the results could not be discussed in this manuscript.

Figure 12 shows the standard gas measurements for the seven cylinders with known CO_2 and O_2 mixing ratios (Table 1) using both the CRDS and the Paramagnetic analyzers. Standard eight, which has too high O_2, is not shown in the figure as the figure is zoomed-in to better illustrate the change in O_2 for the remaining cylinders. While the first five cylinders contain O_2 and CO_2 fractions comparable to ambient air values, standards 6 & 8 had either very low and very high O_2, respectively. In addition, standard 6 and 7 have very low and very high CO_2 mixing ratios. Note that due to its very high CO_2 content (~ 2700 ppm), standard 7 was not measured on the IRMS and hence the O_2 mixing ratios are unknown. The measured mixing ratios for the six standard gases between the two systems are in very good agreement while cylinder 7 showed an opposing signal for the two analyzers compared to standard 6 (Figure 12). While the Paramagnetic analyzer showed a higher O_2 mixing ratio, the values from the CRDS analyzer are lower in O_2. This can be associated with the very high CO_2

454 mixing ratio in standard 7, which leads to a strong dilution effect in the CRDS analyzer as it
455 does not include any correction function for dilution effect from CO_2. However, such high
456 CO_2 mixing ratios may not be that important for most atmospheric research. Yet, it should be
457 considered to include a parallel CO_2 mixing ratios measurement to the instrument as it will
458 further improve the accuracy. This would be especially important for biological or
459 physiological studies where a wide range of CO_2 and O_2 concentrations must be expected.

460 The measurement precision of the CRDS analyzer was calculated as the standard error
461 of the mean i.e. the standard deviation (1-σ) of the last 1-minute raw measurements divided
462 by the square root of the number of measurements (n = 60), and for all these cylinders the
463 values are usually between 0.5 ppm to 0.7 ppm. For parallel measurements of these cylinders
464 using a Paramagnetic analyzer, we obtained a precision of about 1 ppm, calculated exactly the
465 same way.

466 We also made a correlation plot to see which of the two instruments are in better
467 agreement with the assigned values based on IRMS measurements for the individual
468 cylinders. While similar correlation coefficients were observed for both analyzers, different
469 slopes were calculated (Fig. A.1). This is due to the fact that the IRMS measures the O_2 to N_2
470 ratio ($\delta(O_2/N_2)$) in per meg, while the CRDS and the Paramagnetic analyzers provide non-
471 calibrated O_2 mixing ratios in units of ppm and per meg, respectively. If we exclude the two
472 standard gases with the highest and lowest O_2 mixing ratios (standards 7 and 8) that are
473 subjected to strong dilution effects, both the slope and the r^2 values decrease from those
474 shown in Figure A.1. But this decrease is larger in the case of the Paramagnetic
475 measurements, implying a slightly better linearity of the CRDS analyzer.

476 3.2.2. Measurements of ambient air

Ambient air measurements were conducted from the roof top of our laboratory at the University of Bern to evaluate the analyzer's performance under atmospheric variability. Ambient air was continuously aspirated from the inlet at the roof of the building at a flow rate of ~ 250 ml min^{-1} which is then dried using a cooling trap kept at -90 °C towards the switching valve (V1) and measured in similar way to the standard gases as explained above. The measurement values obtained here were compared with the parallel measurements by the Paramagnetic sensor to test the instruments stability and accuracy.

Figures 13 panels a &b show the 1-minute average ambient air measurements from the rooftop inlet by the Paramagnetic and the CRDS analyzers at the beginning of the testing period including standard gases measured every 12-hour. While the Paramagnetic analyzer seems to be stable, the CRDS analyzer showed a strong drift for an extended period. This can be due to unstable conditions in the CRDS measurement system as it started operating right after it was unpacked. Hence, we looked into temperature inside the instrument chassis~~its DAS temperature~~ and pressure records, which were stable within the manufacturer's recommended range during this period. As the CRDS analyzer incorporates a water correction function, interference from this species should be well accounted. Even comparing the analyzer's parallel water measurements to water measurements by the NDIR system such a drift was not observed. It should be noted that the two internal standard gases which were less frequently measured (every 12 hours) during this period were also drifting in similar pattern. This implies that the drift is associated with the analyzer. Interestingly, we observed that the two cylinders follow exactly the same drift pattern that can be modeled using a polynomial function which can then be used to correct for the observed drift in the ambient air measurements. After applying a polynomial drift correction, we were able to fully account for the observed drift. However, the manufacturer decided to further investigate possible causes

Formatted: English (United States)

of this drift. After further improvements, we obtained the first commercial analyzer in September 2017 and repeated the above tests (Figure 13 c &d). No such drift was observed any more in the standard gases or in ambient air measurements.

A possible hypothesis for the cause of the drift can be an optical amplifier in the first system and not anymore included in the design of the product which produced a significant amount of broadband light that could fill the cavity (albeit with a low coupling coefficient), and would ring down with a different (and generally much faster) time constant that the baseline loss of the cavity. However, the ringdown time on the peak of the oxygen line is just 10 microseconds, such that the broadband light might have distorted the single exponential decay of the central laser frequency, leading to the observed drift in the oxygen signal. However, we were not able to confirm this hypothesis.

3.2.3. Water correction test

Measurements of oxygen are reported as both wet ($O_{2,\ raw}$) and dry ($O_{2,\ dry}$) mole fractions by the CRDS analyzer as it also measures water vapor in parallel at its water absorption line (7817 cm^{-1}), and corrects for the dilution effect based on an inbuilt numerical function:

$$O_{2,dry} = \frac{O_{2,raw}}{1 - f_{H_2O}} \qquad (45)$$

where f_{H2O} is the measured water mole fraction.

The efficiency of water correction by this function was assessed in two ways: i) by comparing the water vapor content in standard air measured by this analyzer with similar measurements by the NDIR analyzer and ii) by comparing the oxygen mixing ratios between non-dried

ambient air measured and corrected for water dilution by the CRDS analyzer with dried air measured using a paramagnetic analyzer.

Figure 14 shows the water vapor content for standard gases measured continuously for two days by the CRDS and the NDIR analyzers. Note that the two data sets are manually fitted to each other as the measured water values by the NDIR analyzer are not calibrated. Based on these plots, the two analyzers are in very good agreement although there are small differences during very dry conditions (low water content).

The water correction test was conducted by measuring dried ambient air (Figure 15a) into both analyzers as well as allowing non-dried air to the CRDS analyzer only (Figure 15b) and comparing the difference in O_2 measurements in both cases. (Figures 15c & 15d). shows the water contents of dried ambient air measured in both analyzers while Figure 15b shows in case non-dried air is admitted to the picaro analyzer only (note that the CRDS uses its in-built water correction function). The measurements of the Paramagnetic analyzer were scaled to ppm units by applying the correlation equation obtained from the six standard gas measurements of the two analyzers (Fig. A.1). Note that the CRDS measurements were corrected for the observed drift using the polynomial fit to the two standard gas measurements stated above.

In the first period of the measurement when both analyzers measured dried ambient air, the absolute differences between the 1-minute averages measured over two days by the two analyzers were mostly within 15 ppm and symmetrically distributed around zero. However, when wet air was admitted to the CRDS analyzer and the in-built water correction was applied, a stronger variability was observed in the calculated differences. This implies stronger short term variability in the CRDS analyzer measurement values (as nothing was changed for the Paramagnetic measurement system) when wet samples were analyzed. The

547 more negative values in the differences can also be associated with overestimation of the O_2
548 mixing ratios by the CRDS originating from an overestimated water correction. However,
549 detailed evaluation of the analyzer's water correction function is beyond the scope of this
550 study.

551 **3.3. Field Measurements**

552 After a series of tests at University of Bern, we conducted multiple field measurements
553 at the High Altitude Research Station Jungfraujoch and the Beromünster tall tower sites in
554 Switzerland described below.

555 3.3.1. Tests at the High Altitude Research station Jungfraujoch

556 The High Alpine research station Jungfraujoch is located on the northern ridge of the
557 Swiss Alps (46° 33′ N, 7° 59′ E) at an elevation of 3580 m a.s.l. It is one of the global
558 atmospheric watch (GAW) stations well-equipped for measurements of numerous species and
559 aerosols. The site is above the planetary boundary layer most of the time due to its high
560 elevation (Henne et al., 2010; Zellweger et al., 2003). However, thermally uplifted air from
561 the surrounding valleys during hot summer days or polluted air from the heavily industrialized
562 northern Italy may reach at this site (Zellweger et al., 2003). The Division of Climate and
563 Environmental Physics at the University of Bern has been monitoring CO_2 and O_2 mixing
564 ratios at this site based on weekly flask sampling and continuous measurements since 2000
565 and 2004, respectively (Schibig et al., 2015). The CO_2 mixing ratio is measured using a
566 commercial NDIR analyzer (S710 UNOR, SICK MAIHAK) while O_2 is measured using the
567 Paramagnetic sensor (PM1155 oxygen transducer, Servomex Ltd, UK) and fuel cells (Max-
568 250, Maxtec, USA) embedded within a home-built controlling unit. Similar to the comparison
569 tests at the University of Bern, we have conducted parallel measurements between the CRDS
570 analyzer and the paramagnetic cell at this high altitude site during 03 – 14 February 2017. The

measurement of ambient air at the Jungfraujoch system is composed of sequential switching between a low span (LS) and high span (HS) calibration gases followed by a target gas (T) measurement (once a day) to evaluate the overall system performance and finally a working gas (WG) measurement before switching back to ambient air.

Figure 16 (top panel) shows the calibrated 1-minute averaged O_2 mixing ratios measured at this high altitude site in comparison with the Paramagnetic oxygen analyzer already available at the site. While a strong variability was observed during the measurement period of 10-days by both analyzers, a very good agreement was observed between them.

Figure 16 (bottom panel) shows the absolute difference of 1-minute averages in atmospheric O_2 measured at Jungfraujoch between the two analyzers which are mostly within ±5 ppm range (but sometimes going as high as ±10 ppm) without an offset. However, for generally reported 10-minutes, half-hourly or hourly means these values correspond to < 1.5 ppm, < 1 ppm and < 0.65 ppm.

3.3.2. Tests at the Beromünster tall tower site

The Beromünster tower is located near the southern border of the Swiss Plateau, the comparatively flat part of Switzerland between the Alps in the south and the Jura mountains in the northwest (47° 11′ 23″ N, 8° 10’ 32″ E, 797 m a.s.l.), which is characterized by intense agriculture and rather high population density. A detailed description of the tower measurement system as well as a characterization of the site with respect to local meteorological conditions, seasonal and diurnal variations of greenhouse gases, and regional representativeness can be obtained from previous publications (Berhanu et al., 2016; Berhanu et al., 2017; Oney et al., 2015; Satar et al., 2016). The tower is 217.5 m tall with access to five sampling heights (12.5 m, 44.6 m, 71.5 m, 131.6 m, 212.5 m) for measuring CO, CO_2, CH_4 and H_2O using Cavity Ring Down Spectroscopy (Picarro Inc., G-2401). By sequentially

595 switching from the highest to the lowest level, mixing ratios of these trace gases were
596 recorded continuously for three minutes per height, but only the last 60 seconds were retained
597 for data analysis. The calibration procedure for ambient air includes measurements of
598 reference gases with high and low mixing ratios traceable to international standards (WMO-
599 X2007 for CO_2 and WMO-X2004 for CO and CH_4), as well as target gas and more frequent
600 working gas determinations to ensure the quality of the measurement system. From two years
601 of data a long-term reproducibility of 2.79 ppb, 0.05 ppm, and 0.29 ppb for CO, CO_2 and
602 CH_4, respectively was determined for this system (Berhanu et al., 2016).

603 Between 15.02.2017 and 02.03.2017, we have connected the new CRDS oxygen
604 analyzer in series with the CO_2 analyzer (Picarro G-2401) and measured the O_2 mixing ratios
605 at the corresponding heights. Similar to the CO_2 measurements, O_2 was also measured for
606 three minutes at each height. During this period, we have evaluated the two features (isotopic
607 mode and concentration mode) of the CRDS analyzer. In the isotopic mode, the CRDS
608 measures the $\delta^{18}O$ values as well as the O_2 concentration while in concentration mode only
609 the latter was measured.

610 During the tests conducted at this tower site, we first evaluated the two operational
611 modes (concentration vs isotopic modes) of the CRDS analyzer. Ambient air measurements
612 on isotopic mode over a 4-days period showed a strong variability in the measured oxygen
613 mixing ratios and it was not possible to distinguish the variability in the O_2 mixing ratios
614 among the five height levels. The calculated 1-minute standard error for ambient air
615 measurements was as high as 10 ppm while a standard error of less than 1 ppm was
616 determined from similar measurements in the concentration mode. Additionally, comparing
617 the O_2 values between the two modes, frequent short time variation in ambient air O_2 (~ 200
618 ppm) was observed in the isotope mode measurements while the variation in the concentration

mode is significantly smaller (~ 30 ppm). This precision degradation is due to the weaker ^{16}O oxygen line used for the isotopic mode, and the fact that far more ring-downs are collected on the rare isotopologue in isotopic mode Hence, we have conducted the remaining test measurements in concentration mode.

As this tower has five sampling height levels, we first followed three minutes of switching per inlet level, which enables four measurements per hour at a given level. However, we noticed hardly any difference among the different levels due to strong short term variability in O_2 mixing ratios between the consecutive heights. Hence, we switched to a longer sampling period of six-minutes per height. Figure 17 shows the diurnal CO_2 and O_2 variations at the lowest (12 m) and highest (212.5 m) sampling heights of the tower. These two heights were selected simply to better illustrate the difference in the mixing ratios. The CO_2 mixing ratios on the top panel show higher values at the 12 m inlet than the highest level most of the day due to its closeness to sources except during the afternoon (11:00 - 17:00 UTC) when both levels show similar but decreasing CO_2 mixing ratios. This is due to presence of a well-mixed planetary boundary layer (PBL) (Satar et al., 2016). The lag in CO_2 peak between the two height levels by about two hours indicates the duration for uniform vertical mixing along the tower during winter 2017. The opposite variability patterns are also clearly visible in the O_2 mixing ratios shown in the lower panel with a clear distinction between the two height levels during early in the morning and in the evening while similar O_2 values were observed in the afternoon. These opposing profiles are expected as CO_2 and O_2 are linearly coupled with a mean oxidation ratio of -1.1 ± 0.05 (Severinghaus, 1995) for land-biospheric processes (photosynthesis and respiration) and -1.44 ± 0.03 for fossil fuel burning (Keeling, 1988b).

642 Table 2 shows the oxidation ratios derived as the slopes of the linear regression
643 between CO_2 and O_2 mixing ratios at the different height levels measured on 25 February
644 2017. Accordingly, height dependent slopes were observed with a slope of -0.98 ± 0.06 at the
645 lowest level, close to the biological processes induced slope but slightly lower than its mean
646 value. For the highest level, we calculated a slope of -1.60 ± 0.07 a value close to fossil fuel
647 combustion oxidation ratio. Note that depending on fossil fuel type the oxidation ratio can
648 range between -1.17 and -1.95 for coal and natural gas, respectively (Keeling, 1988b). While
649 the slopes derived for the two other levels (44.6 m and 131.6 m) show similar values between
650 the highest and lowest height levels, possibly from mixed sources, the middle level showed a
651 slightly higher slope than these two levels but still in the large range between the lowest and
652 highest inlet heights.

653 3.4. Evaluation of the $\delta^{18}O$ measurements

654 To further evaluate the analyzer's performance in measuring stable oxygen isotopes,
655 we conducted ambient air isotopic composition measurements as well as analyzed a standard
656 gas without CO_2 which has a known $\delta^{18}O$ value. The choice of this CO_2-free air standard gas
657 is twofold: one it has a known $\delta^{18}O$ value and second as it has no CO_2 possible interference
658 from band overlap ~~is avoided~~. For this test three 0.5 L glass flasks were preconditioned and
659 filled with this standard gas to ambient pressure. These flasks were attached before or after
660 the water trap (Fig. 11) and measured similar to ambient air measurements. These
661 measurements were then compared with $\delta(^{34}O/^{32}O)$ values obtained by parallel measurements
662 using our IRMS.

663 Figure 18 shows the $\delta^{18}O$ values of ambient air from the roof top with three
664 consecutive measurements of glass flasks filled with CO_2-free air in-between followed by a
665 fourth flask filled with breath air. An excellent agreement was observed for measurements

from both instruments for the three flasks filled with a standard gas. However, the fourth flask with breath air showed a signal opposite to the measurements by the IRMS. As breath air contains large amount of water and CO_2 in addition to O_2, which can possibly interfere with the CRDS analyzer measurements, we have removed H_2O and CO_2 by using a cryogenic trap (-130 °C) and in an additional experiment using Schütze reagent to remove both CO and CO_2. However, we have not observed any improvement towards an agreement with the IRMS measurements. Therefore, any other gas component in the breath air must be relevant for the interference. Based on the absorption lines in the spectral range of the instrument (7878 cm^{-1}) retrieved from HITRAN database, we expect interference either from carbon monoxide (now excluded by the tests) or methane or VOCs including acetone, ethanol, methanol or isoprenes, all of which have been measured in breath air (Gao et al., 2017; Gottlieb et al., 2017; Mckay et al., 1985; Ryter and Choi, 2013; Wolf et al., 2017). Further investigations have to shed light on these interferences in order to take corresponding action to surpass these shortcomings in the isotope analysis based on cavity ring-down spectroscopy.

4. Conclusions

We have thoroughly evaluated the performance of a new CRDS analyzer which measures O_2 mixing ratios and isotopic composition combining laboratory and field tests. Even if a drift in the analyzer was observed at the beginning of this study, which if it appears can be easily corrected by calibration, the recent analyzers built by the manufacturer did not show such instrumental drift. However, prior tests are recommended to see the analyzer's stability.

The T-split tests for the current measurement setup based on the measurements of two standard gases showed a difference within the measurement uncertainty. However, this effect

689 may become significant while applying larger splitting ratios and we recommend conducting
690 further experiments to accurately quantify this influence for larger splitting ratios.

691 We have observed a strong influence of dilution in the measured O_2 values during the
692 presence of high CO_2 mixing ratios. Even if such an influence may not be critical for the
693 present study, such an effect might be significant in other studies where higher CO_2 mixing
694 ratios might be present and we recommend following a correction strategy based on parallel
695 CO_2 measurements. This also applies for more accurate analysis.

696 The water correction applied by the instrument's in-built function seems to sufficiently
697 correct for the water vapor influence. However, a larger variability of the difference was
698 observed between the CRDS analyzer and the Paramagnetic cell when dried samples were
699 used in both systems. This can possibly be due to an overcorrection by the water correction
700 function of the CRDS analyzer when dried samples were used. This is particularly true for the
701 very low water vapor range (< 100 ppm). However, we believe that it is important to further
702 investigate this issue and identify an improved water correction strategy.

703 Based on the analysis of O_2 mixing ratios in the concentration and isotopic modes, we
704 have observed about a significant decrease in precision (about ten-fold) in the latter
705 measurement mode. The measured $\delta^{18}O$ values for the standard air by the CRDS analyzer are
706 in excellent agreement with the IRMS values. However, such measurements for a breath air
707 showed a contrasting signal, possibly due to interference from other gases as breath air
708 contains CO_2, CH_4 and CO in addition to oxygen. Hence, we recommend further investigation
709 on such possible contaminants and how to possibly remove them while conducting ambient
710 air measurements. However, we believe that this analyzer can be used for tracer experiments
711 where artificially enriched isotopes are used to study biological processes such as
712 photosynthesis in plants using isotopically labelled CO_2 and H_2O.

Acknowledgement

We would like to thank ICOS-RI and the Swiss National Science Foundation (SNF) for funding ICOS-CH (20FI21_148994, 20FI21_148992). We are also grateful to the International Foundation High Alpine Research Stations Jungfraujoch and Gornergrat. The measurement system at the Beromünster tower was built and maintained by the CarboCount-CH (CRSII2_136273) and IsoCEP (200020_172550) projects both funded by SNF.

List of Tables

Table 1. Assigned mixing ratios of standard gases used in this study and their corresponding values measured by the NDIR, CRDS and IRMS at the University of Bern. [1]The assigned values are based on measurements from different institutions (University of Bern (UB), Scripps or NOAA, see column cylinder name). [2]Measurements are on the Bern scale for CO_2 and O_2. The Bern scale is shifted by +550 per meg. [3]Values on the Scripps scale.

737

Cylinder name	Assigned CO_2 (ppm) [1]	Assigned O_2 (per meg) [1]	CO_2-IRMS (ppm) [2]	CO_2-NDIR (ppm) [2]	O_2-IRMS (per meg) [2]	O_2-Paramagnetic (per meg) [2]	O_2-CRDS (per meg)[2]
ST-1 LUX3576-UB	427.47	-1026	427.47	427.59	-1026	-1070	-1057
ST-2 LK922131-UB	368.09	599	368.09	367.82	599	560	590
ST-3 CA07045-Scripps	382.303	-271.6	382.50	381.99	278 (-272.2)[3]	302	281
ST-4 CA07043-Scripps	390.528	-476.4	390.69	390.15	71 (-479.5)[3]	66	63
ST-5 CA07047-Scripps	374.480	-807.7	374.70	374.17	-253 (-803.3)[3]	-212	-233
ST-6 CA04556-NOAA	192.44	-3410	191.21	191.64	-3410	-2905	-3013
ST-7 CA06943-NOAA	2699.45	-		2612.80	-	-2691	-3369
ST-8 LK76852-UB	411.49	37794	411.49	406.25	37794	34513	36017

738

739

740 Table 2. The CO_2 and O_2 correlation coefficients at the different height levels derived using
741 the least square fit and the correlation coefficients (r^2). Uncertainties are calculated as
742 standard error of the slope.

Height	Oxidation Ratios (O_2:CO_2)
12.5 m	-0.98 ± 0.06 (0.48)
44.6 m	-1.29 ± 0.07 (0.50)
71.5 m	-1.49 ± 0.08 (0.47)
131.6 m	-1.23 ± 0.05 (0.55)
212.5 m	-1.60 ± 0.07 (0.61)

743
744
745
746
747
748
749
750
751 List of Figures

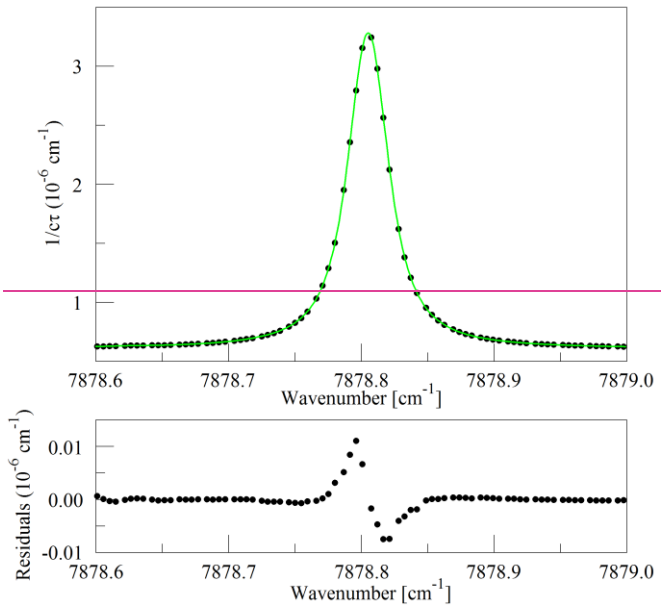
3
2
1
1/cτ (10^-6 cm^-1)
7878.6
7878.7
7878.8
7878.9
7879.0
Wavenumber [cm^-1]
0.01
0.00
-0.01
Residuals (10^-6 cm^-1)
7878.6
7878.7
7878.8
7878.9
7879.0
Wavenumber [cm^-1]

752

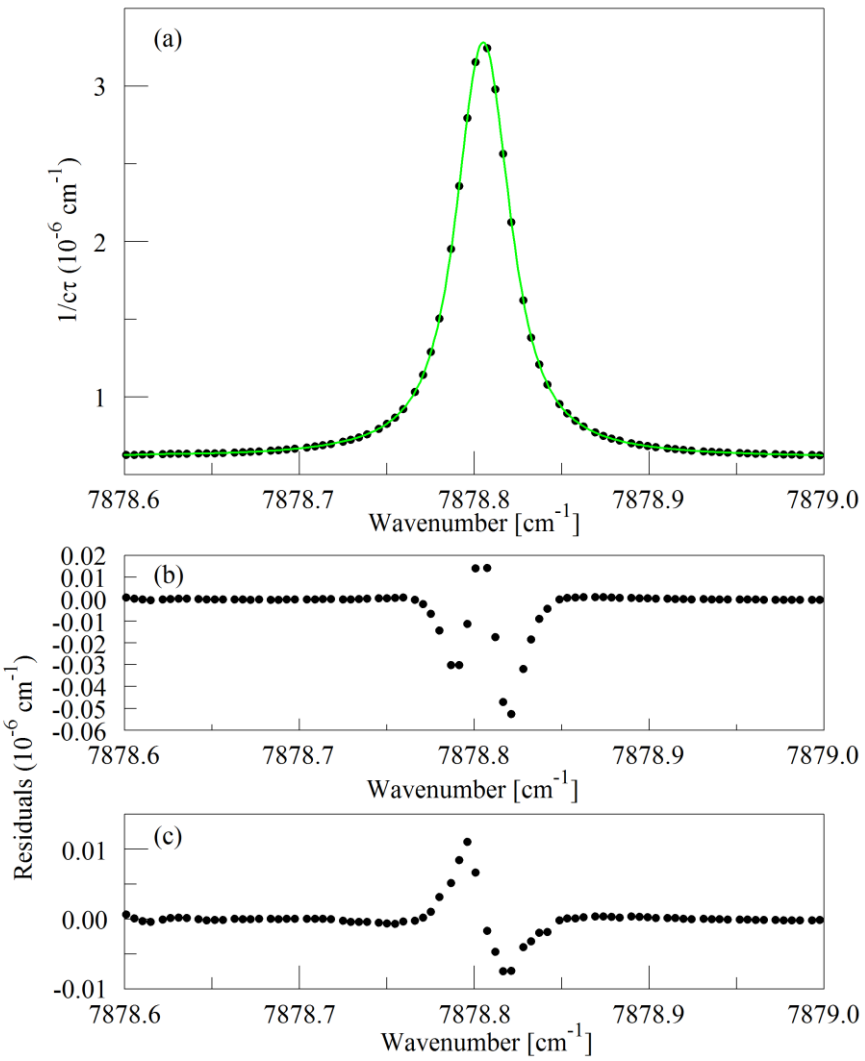

753

754 Figure 1. ~~The Q13Q13 line of O_2 measured in a sample of synthetic air at a sample~~

755 ~~temperature and pressure of 45° C and 333 hPa, respectively.~~

756 The top panel (a) shows the raw data (points) and the best-fit Galatry function (solid line). Residuals

757 of the Voigt fit are shown in panel (b) and residuals of the Galatry fit are shown in panel (c)

Formatted: English (United States)

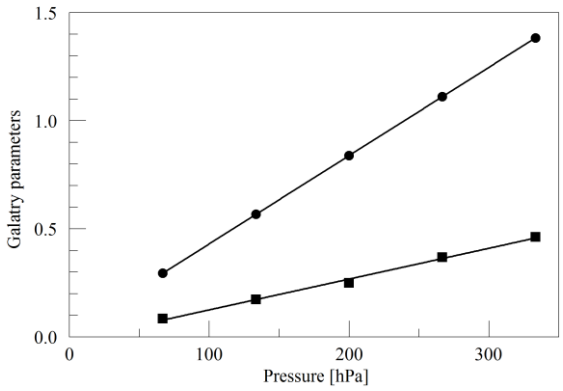

Figure 2. Best-fit values for the Galatry parameters of the Q13Q13 line of O_2, as a function of pressure. The line broadening parameter y is represented by circles and the line narrowing parameter z by squares. The solid lines are linear fits to the measurements. The best-fit offset and slope are 0.0227 and 0.004082 hPa^{-1} for y, and -0.0169 and 0.001424 hPa^{-1} for z.

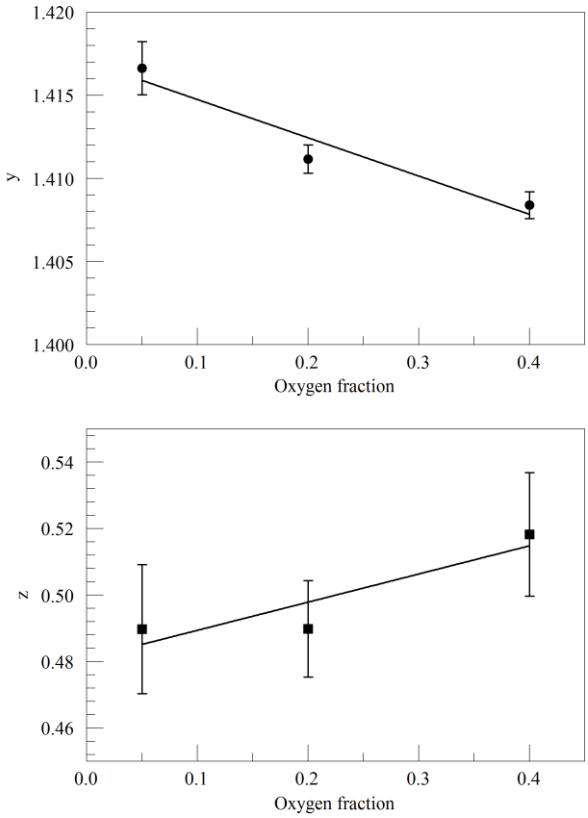

772

773 Figure 3. Galatry parameters of the Q13Q13 line of O_2 at 340 hPa and 45° C as a function of

774 O_2 mole fraction in binary O_2 - N_2 mixtures.

775 The linear fits to the data are $y = 1.417 – 0.023 \times f_{O2}$ and $z = 0.481 + 0.085 \times f_{O2}$.

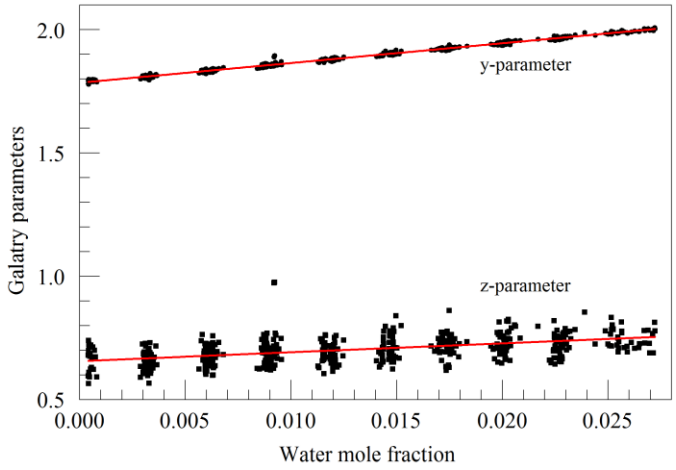

Figure 4. Galatry parameters of the 7816.75210 cm^{-1} water line in air at 340 hPa and 45° C as a function of water mole fraction. Black points are from measurements and red lines are linear fits: $y = 1.7846 + 8.01 \times f_{H2O}$ and $z = 0.656 + 3.60 \times f_{H2O}$.

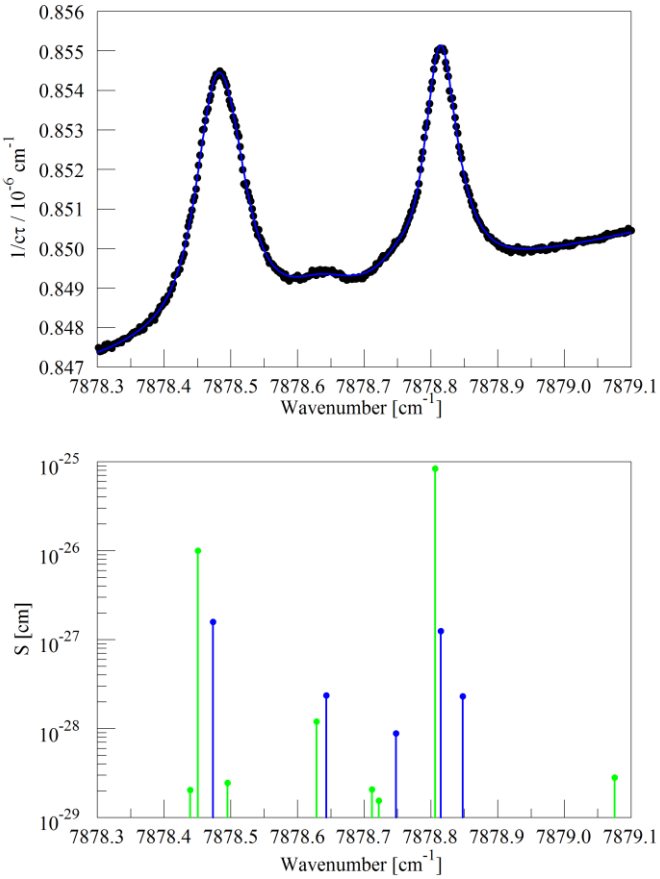

780

781 Figure 5. Upper panel: spectrum of water in nitrogen (points) and fit to Voigt model (blue

782 curve). Lower panel: Oxygen (green) and water (blue) lines in the Hitran database.

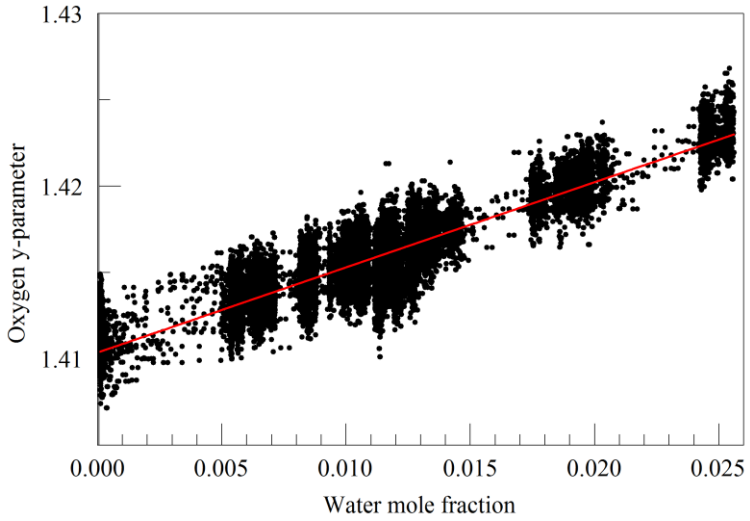

Figure 6. Galatry collisional broadening parameter of the oxygen Q13Q13 line at 340 hPa and 45° C versus water mole fraction. Black points are from measurements and the red line is a linear fit: $y = 1.4109 + 0.467\ f_{H2O}$.

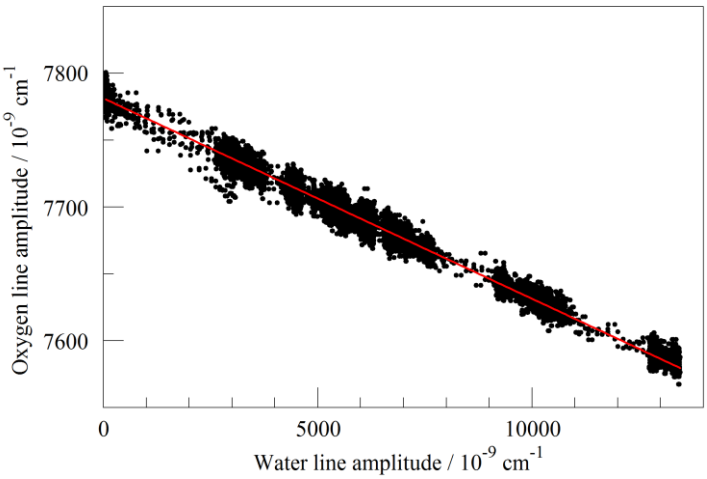

Figure 7. Measured absorption line amplitudes for oxygen and water vapor for water vapor mixing ratios ranging from nearly 0 to 0.025. Black points are from measurements and the red line is a linear fit: with intercept 7.78001 x 10^{-6} cm^{-1} and slope -0.014807.

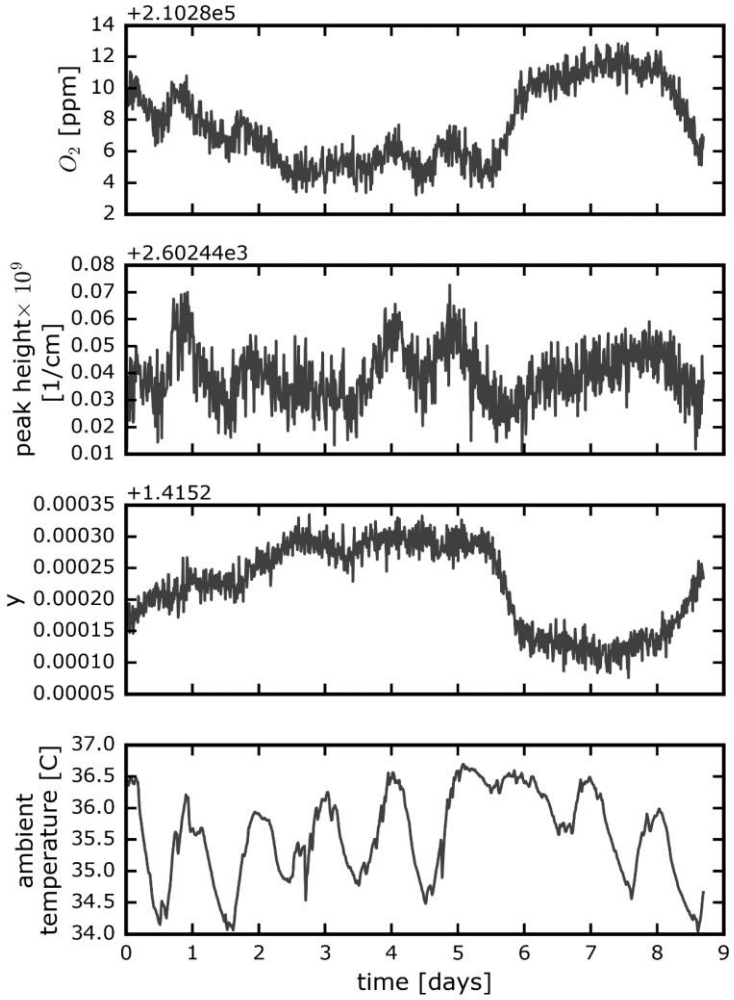

Figure 8. Time series from a measurement of a single tank over about a week. The four panels show~~n~~ the water-corrected oxygen concentration, the absorption peak loss minus the baseline loss, the measured Lorentzian broadening factor, and the ambient temperature (measured in the instrument housing), respectively. A windowed average of 300 seconds was applied to all four data sets.

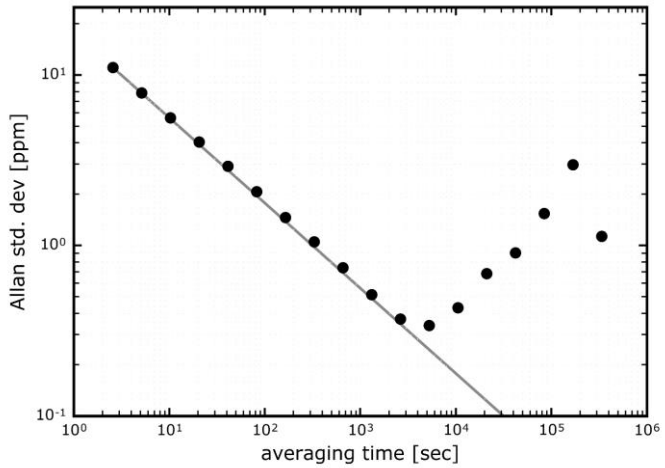

Figure 9. Precision of O_2 mole fraction measured from a tank of synthetic air. Filled circles are measurements and the line shows the ideal $\tau^{-1/2}$ dependence.

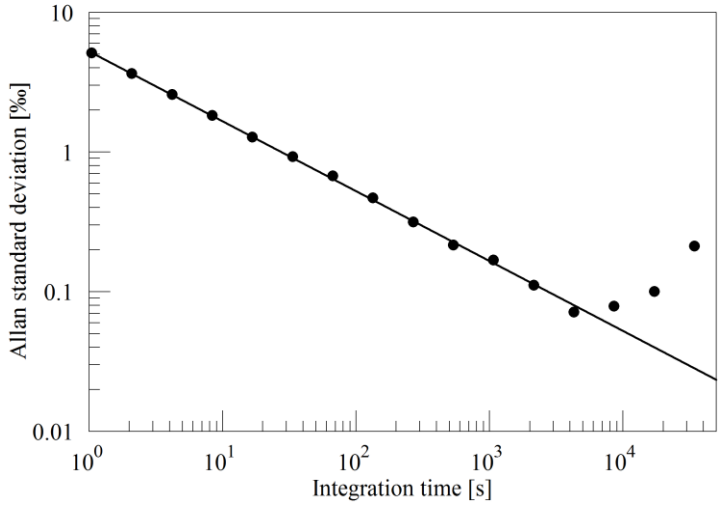

Figure 10. Precision of $\delta(^{18}O)$ measured from a tank of synthetic air. Filled circles are measurements and the line shows the ideal $\tau^{-1/2}$ dependence.

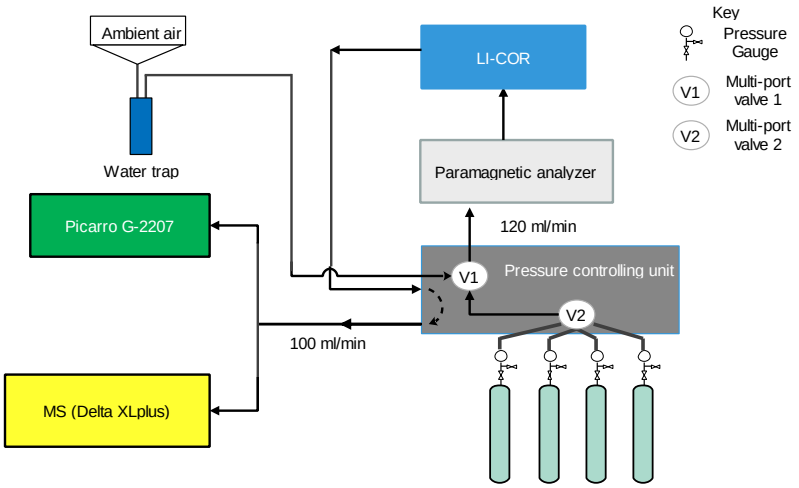

826

827 Figure 11. Schematics of the measurement system used to compare the Picarro analyzer with

828 the Mass Spectrometer at Bern.

829

830

831

832

833

834

835

836

837

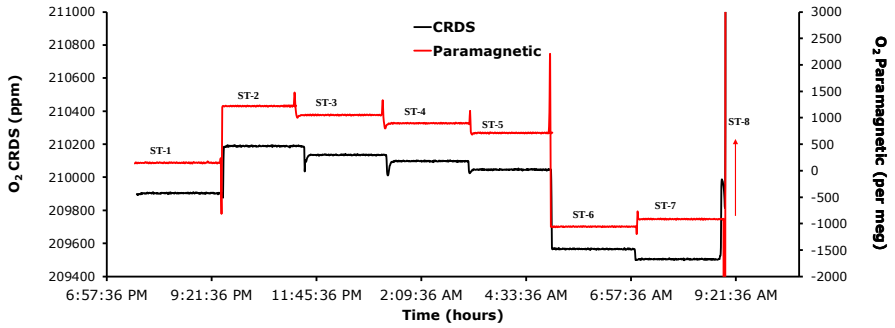

838

839 Figure 12. Comparison of oxygen mixing ratios for the seven standard gases measured using

840 the CRDS analyzer (black) and the Paramagnetic sensors (red).

841

842

843

844

845

846

847

848

849

850

851

852

853

854

855

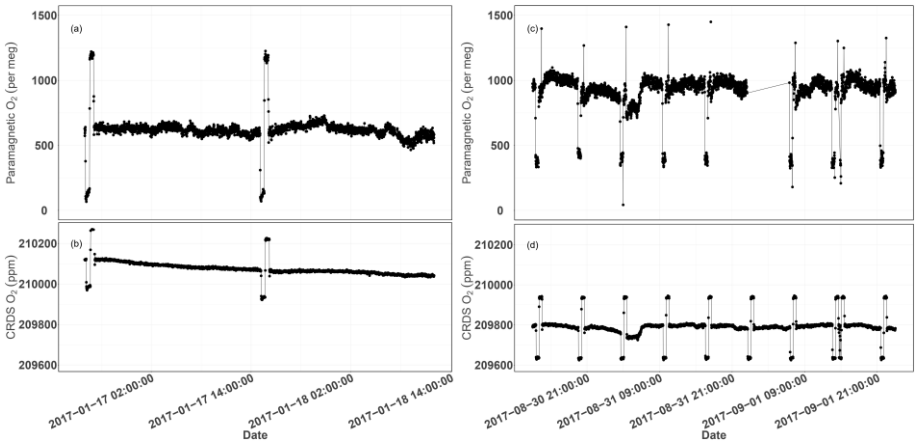

Figure 13. Parallel ambient air measurements by the Paramagnetic and CRDS analyzers at the beginning of the testing period (Panels a & b, January 2017) and the second phase of testing (Panels c & d, September 2017). The spikes are measurements from the two standard gases bracketing the ambient air values.

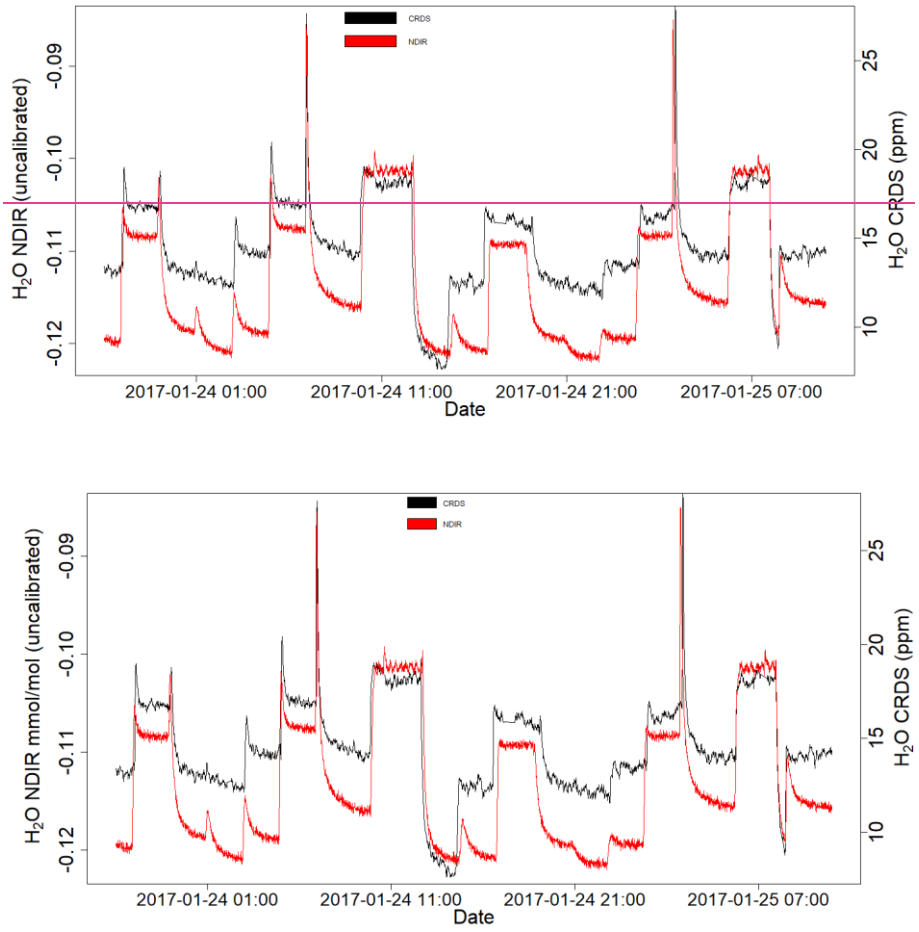

Figure 14. Parallel water vapor measurements for a dried ambient air by both the NDIR and CRDS analyzers. Note that the water values from the NDIR analyzer are not calibrated.

881

882

883

884

885

886

887

888

889

890

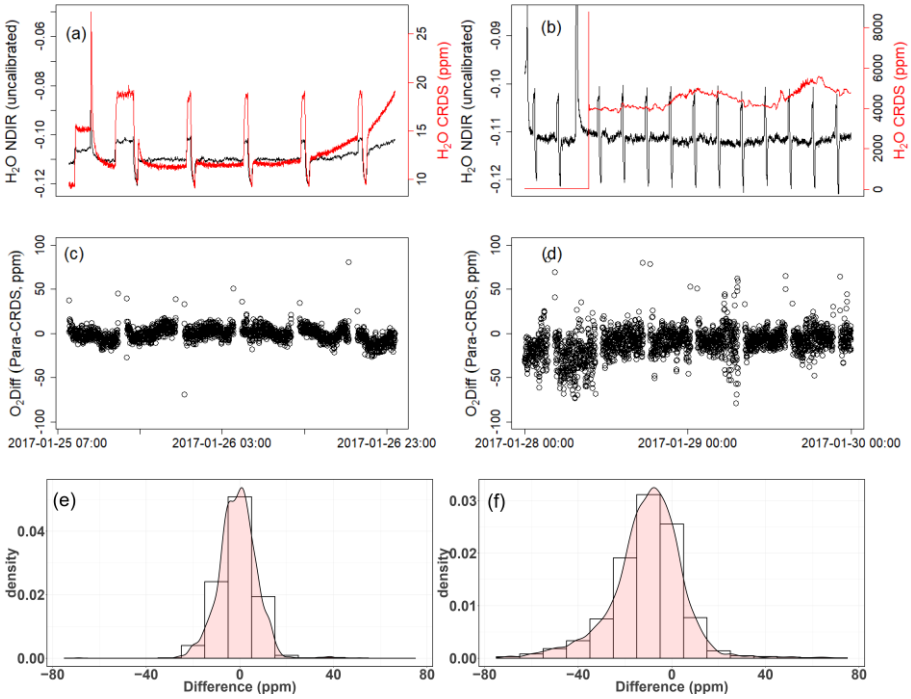

Figure 15. Results of water correction tests. Water measurements of the NDIR (left scale) for dry conditions (a,b) and the CRDS analyzer (right scale) for dry (a) and wet (b) conditions. The difference in oxygen measurements between the Paramagnetic and the CRDS instrument using the built-in water correction for the CRDS values under dry (c) and wet (d) conditions. Panels (e) and (f) show the population density functions.

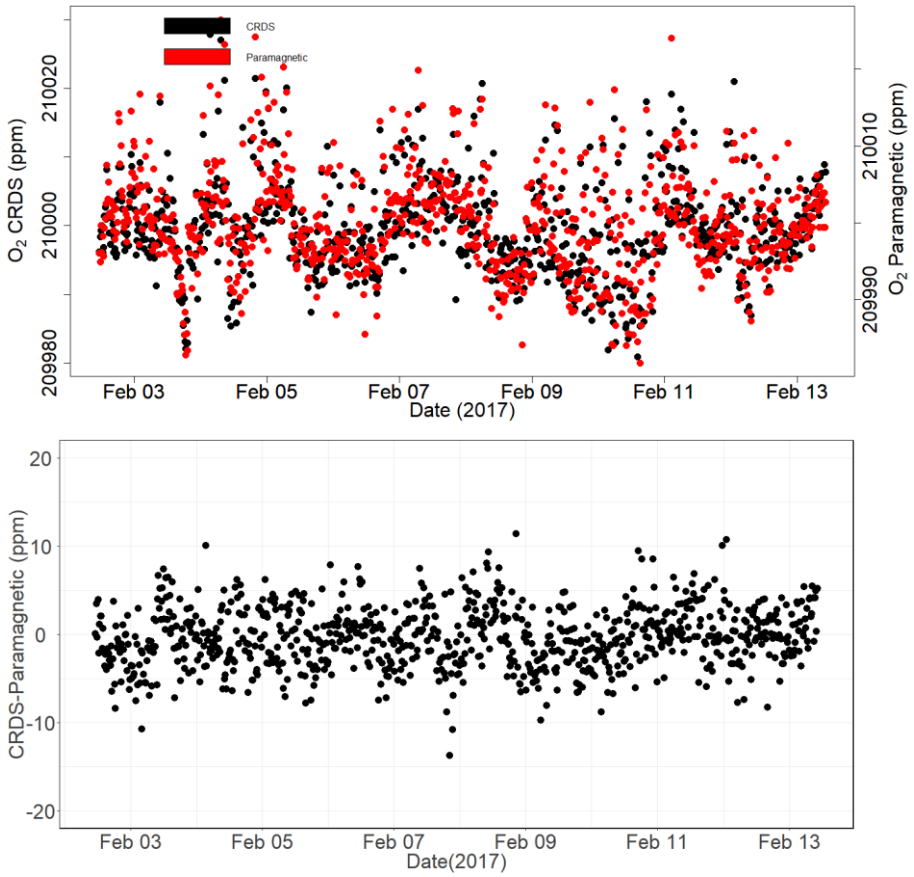

Figure 16. Calibrated ambient air oxygen measurements (1-minute average) at the Jungfraujoch site using the CRDS and Paramagnetic analyzers both in ppm units (a) and the absolute difference between the two measurements in ppm (b) by matching time stamps.

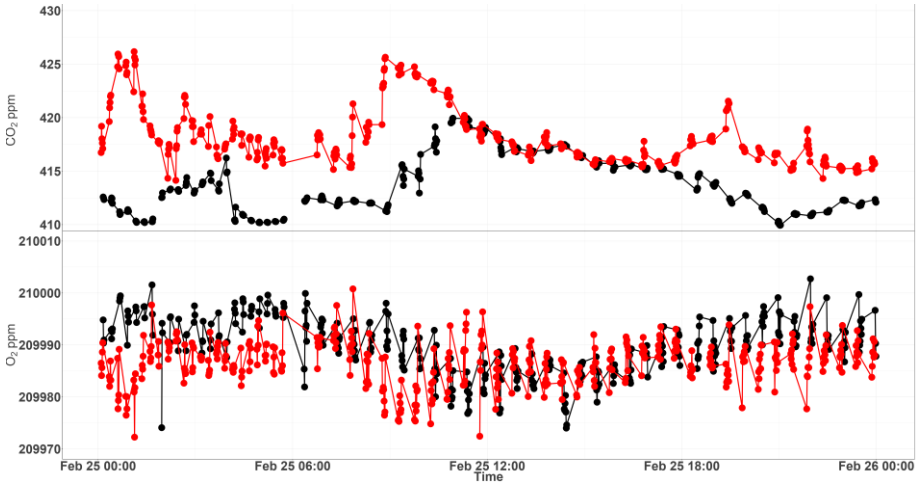

Figure 17. Diurnal variations of CO_2 (top) and O_2 (bottom) measurements from the 12 m (red) and the 212.5 m (black) height levels at Beromünster tower.

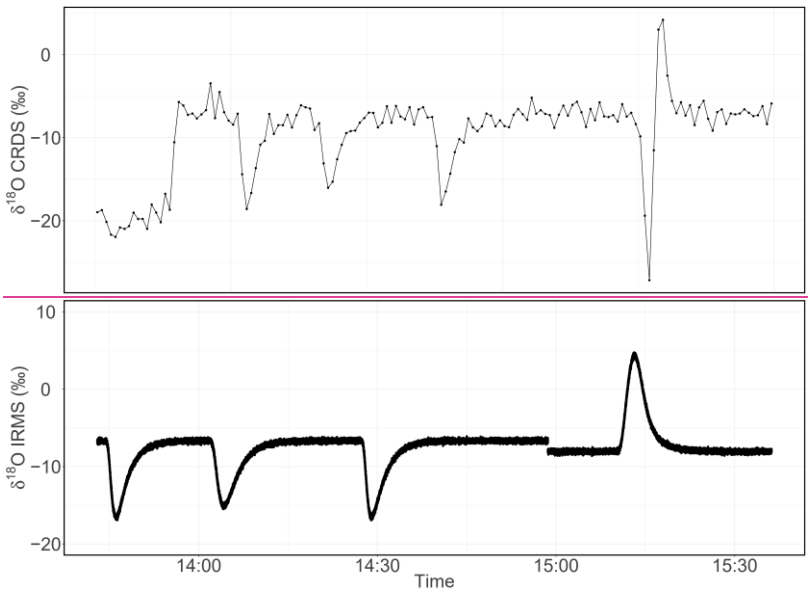
0
−10
−20
δ18O CRDS (‰)
10
0
−10
−20
δ18O IRMS (‰)
14:00
14:30
15:00
15:30
Time

922

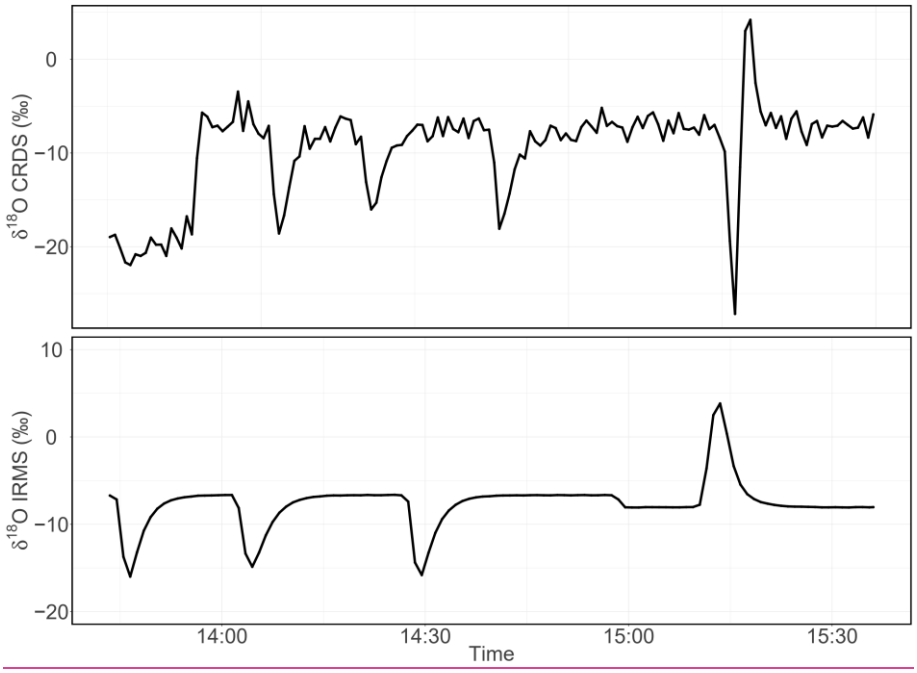
0
−10
−20
δ18O CRDS (‰)
10
0
−10
−20
δ18O IRMS (‰)
14:00
14:30
15:00
15:30
Time

923

Figure 18. Consecutive $\delta^{18}O$ measurements of a standard gas (CO_2-free air) filled into three flasks followed by measurement of breath air using the CRDS analyzer (top) and IRMS (bottom). These measurements were carried out in the middle of ambient air measurements.

Appendix A.

Additional plots

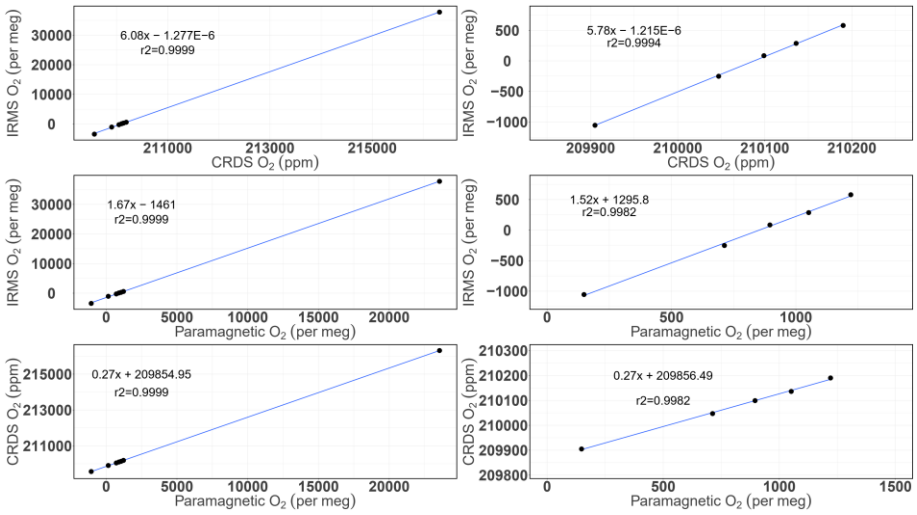

Figure A.1. Correlations between the O_2 mixing ratios measured by the CRDS and Paramagnetic analyzers with the mass spectrometric measurements (uncalibrated values). The left panels are for all the cylinders measured (standards 1 to 8) while the right ones are after zooming only to standards 1-5.

References

953 Battle, M., Bender, M. L., Tans, P. P., White, J. W. C., Ellis, J. T., Conway, T., and Francey, R. J.: Global
954 carbon sinks and their variability inferred from atmospheric O-2 and delta C-13, Science, 287, 2467-
955 2470, 2000.
956 Bender, M. L., Tans, P. P., Ellis, J. T., Orchardo, J., and Habfast, K.: A High-Precision Isotope Ratio
957 Mass-Spectrometry Method for Measuring the O-2 N-2 Ratio of Air, Geochim Cosmochim Ac, 58,
958 4751-4758, 1994.
959 Berhanu, T. A., Satar, E., Schanda, R., Nyfeler, P., Moret, H., Brunner, D., Oney, B., and Leuenberger,
960 M.: Measurements of greenhouse gases at Beromünster tall tower station in Switzerland, Atmos.
961 Meas. Tech. , 9, 2016.
962 Berhanu, T. A., Szidat, S., Brunner, D., Satar, E., Schanda, R., Nyfeler, P., Battaglia, M., Steinbacher,
963 M., Hammer, S., and Leuenberger, M.: Estimation of the fossil-fuel component in atmospheric CO2
964 based on radiocarbon measurements at the Beromünster tall tower, Switzerland, Atmos. Chem.
965 Phys. Discuss., 2017, 1-33, 2017.
966 Crosson, E. R. J. A. P. B.: A cavity ring-down analyzer for measuring atmospheric levels of methane,
967 carbon dioxide, and water vapor, 92, 403-408, 2008.
968 Filges, A., Gerbig, C., Rella, C. W., Hoffnagle, J., Smit, H., KrÃ¤mer, M., Spelten, N., Rolf, C., BozÃ³ki, Z.,
969 Buchholz, B., and Ebert, V.: Evaluation of the IAGOS-Core GHG Package H2O measurements during
970 the DENCHAR airborne inter-comparison campaign in 2011, Atmos. Meas. Tech., 11, 5279–5297,
971 2018, https://doi.org/10.5194/amt-11-5279-2018. ~~Atmos. Meas. Tech. Discuss., doi: 10.5194/amt-~~
972 ~~2018-36, 2018. 2018.~~
973 ~~Fleisher, A. J., Hodges, J., and Sironneau, V.: Collision-dependent line areas in the a1Δg← X3Σ−g band~~
974 ~~of molecular oxygen, 2015.~~
975 Gao, F., Zhang, X., Zhang, X., Wang, M., and Wang, P.: Virtual electronic nose with diagnosis model
976 for the detection of hydrogen and methane in breath from gastrointestinal bacteria, 28-31 May 2017
977 2017, 1-3.

978 Gordon, E., Rothman, S., Hill, C., Kochanov, V., Tan, Y., Bernath, P., Birk, M., Boudon, V., Campargue,
979 A., Chance, K., Drouin, J., Flaud, J., Gamache, R. R., Hodges, J., Jacquemart, D., Perevalov, I., Perrin, A.,
980 Shine, P., Smith, M., Tennyson, J., Toon, G., Tran, H., Tyuterev, G., Barbe, A., Császár, G., Devi, M.,
981 Furtenbacher, T., Harrison, J., Hartmann, J., Jolly, A., Johnson, J., Karman, T., Kleiner, I., Kyuberis, A.
982 A., Loos, J., Lyulin, M., Massie, S., Mikhailenko, S., Moazzen-Ahmadi, N., Muller, S., Naumenko, O. V.,
983 Nikitin, A. V., Polyansky, O. L., Rey, M., Rotger, M., Sharpe, S., Sung, K., Starikova, E., Tashkun, S.,
984 Auwera, J., Wagner, G., Wilzewski, J., Wcisło, P., Yu, S., and Zak, E. J.: The HITRAN2016 molecular
985 spectroscopic database, 203, 3 - 69, 2017.
986 Goto, D., Morimoto, S., Ishidoya, S., Aoki, S., and Nakazawa, T.: Terrestrial biospheric and oceanic
987 CO2 uptake estimated from long-term measurements of atmospheric CO2 mole fraction, δ13C and
988 δ(O2/N2) at Ny-Ålesund, Svalbard, Journal of Geophysical Research: Biogeosciences, doi:
989 10.1002/2017JG003845, 2017. n/a-n/a, 2017.
990 Gottlieb, K., Le, C. X., Wacher, V., Sliman, J., Cruz, C., Porter, T., and Carter, S.: Selection of a cut-off
991 for high- and low-methane producers using a spot-methane breath test: results from a large north
992 American dataset of hydrogen, methane and carbon dioxide measurements in breath, Gastroenterol
993 Rep, 5, 193-199, 2017.
994 Hartmann, J.-M., Boulet, C., and Robert, D.: Collisional Effects on Molecular Spectra, Elsevier Science,
995 2008.
996 Henne, S., Brunner, D., Folini, D., Solberg, S., Klausen, J., and Buchmann, B.: Assessment of
997 parameters describing representativeness of air quality in-situ measurement sites, Atmos. Chem.
998 Phys., 10, 3561-3581, 2010.
999 Hodges, J. T., Layer, H. P., Miller, W. W., and Scace, G. E.: Frequency-stabilized single-mode cavity
1000 ring-down apparatus for high-resolution absorption spectroscopy, 75, 849-863, 2004.
1001 Keeling, R. F.: Development of an Interferometric Oxygen Analyzer for Precise Measurement of the
1002 Atmospheric O2 Mole Fraction, UMI, 1988a.

1003 Keeling, R. F.: Measuring correlations between atmospheric oxygen and carbon dioxide mole
1004 fractions: A preliminary study in urban air, J Atmos Chem, 7, 153-176, 1988b.
1005 Keeling, R. F. and Manning, A. C.: 5.15 - Studies of Recent Changes in Atmospheric O2 Content A2 -
1006 Holland, Heinrich D. In: Treatise on Geochemistry (Second Edition), Turekian, K. K. (Ed.), Elsevier,
1007 Oxford, 2014.
1008 Keeling, R. F. and Shertz, S. R.: Seasonal and Interannual Variations in Atmospheric Oxygen and
1009 Implications for the Global Carbon-Cycle, Nature, 358, 723-727, 1992.
1010 Keeling, R. F., Stephens, B. B., Najjar, R. G., Doney, S. C., Archer, D., and Heimann, M.: Seasonal
1011 variations in the atmospheric O-2/N-2 ratio in relation to the kinetics of air-sea gas exchange, Global
1012 Biogeochem Cy, 12, 141-163, 1998.
1013 Lamouroux, J., Sironneau, V., Hodges, J. T., and Hartmann, J. M.: Isolated line shapes of molecular
1014 oxygen: Requantized classical molecular dynamics calculations versus measurements, Physical
1015 Review A, 89, 042504, 2014.
1016 Le Quéré, C., Andrew, R. M., Friedlingstein, P., Sitch, S., Pongratz, J., Manning, A. C., Korsbakken, J. I.,
1017 Peters, G. P., Canadell, J. G., Jackson, R. B., Boden, T. A., Tans, P. P., Andrews, O. D., Arora, V. K.,
1018 Bakker, D. C. E., Barbero, L., Becker, M., Betts, R. A., Bopp, L., Chevallier, F., Chini, L. P., Ciais, P.,
1019 Cosca, C. E., Cross, J., Currie, K., Gasser, T., Harris, I., Hauck, J., Haverd, V., Houghton, R. A., Hunt, C.
1020 W., Hurtt, G., Ilyina, T., Jain, A. K., Kato, E., Kautz, M., Keeling, R. F., Klein Goldewijk, K., Körtzinger, A.,
1021 Landschützer, P., Lefèvre, N., Lenton, A., Lienert, S., Lima, I., Lombardozzi, D., Metzl, N., Millero, F.,
1022 Monteiro, P. M. S., Munro, D. R., Nabel, J. E. M. S., Nakaoka, S. I., Nojiri, Y., Padín, X. A., Peregon, A.,
1023 Pfeil, B., Pierrot, D., Poulter, B., Rehder, G., Reimer, J., Rödenbeck, C., Schwinger, J., Séférian, R.,
1024 Skjelvan, I., Stocker, B. D., Tian, H., Tilbrook, B., van der Laan-Luijkx, I. T., van der Werf, G. R., van
1025 Heuven, S., Viovy, N., Vuichard, N., Walker, A. P., Watson, A. J., Wiltshire, A. J., Zaehle, S., and Zhu,
1026 D.: Global Carbon Budget 2017, Earth Syst. Sci. Data Discuss., 2017, 1-79, 2017.

1027 Manning, A.: Temporal variability of atmospheric oxygen from both continuos and measurements
1028 and a flask sampling network: tools for studying the global carbon cycle, Ph.D. Ph.D., University of
1029 California, San Diego, San Diego, Calofornia, USA, 2001.
1030 Manning, A. C. and Keeling, R. F.: Global oceanic and land biotic carbon sinks from the Scripps
1031 atmospheric oxygen flask sampling network, Tellus B, 58, 95-116, 2006.
1032 Manning, A. C., Keeling, R. F., and Severinghaus, J. P.: Precise atmospheric oxygen measurements
1033 with a paramagnetic oxygen analyzer, Global Biogeochem Cy, 13, 1107-1115, 1999.
1034 Marrero, T. R. and Mason, E. A.: Gaseous Diffusion Coefficients, Journal of Physical and Chemical
1035 Reference Data 1, 3, 1972.
1036 Martin, N. A., Ferracci, V., Cassidy, N., and Hoffnagle, J. A. J. A. P. B.: The application of a cavity ring-
1037 down spectrometer to measurements of ambient ammonia using traceable primary standard gas
1038 mixtures, 122, 219, 2016.
1039 Mckay, L. F., Eastwood, M. A., and Brydon, W. G.: Methane Excretion in Man - a Study of Breath,
1040 Flatus, and Feces, Gut, 26, 69-74, 1985.
1041 Nevison, C. D., Keeling, R. F., Kahru, M., Manizza, M., Mitchell, B. G., and Cassar, N.: Estimating net
1042 community production in the Southern Ocean based on atmospheric potential oxygen and satellite
1043 ocean color data, Global Biogeochem Cy, 26, 2012.
1044 Oney, B., Henne, S., Gruber, N., Leuenberger, M., Bamberger, I., Eugster, W., and Brunner, D.: The
1045 CarboCount CH sites: characterization of a dense greenhouse gas observation network, Atmos.
1046 Chem. Phys., 15, 11147-11164, 2015.
1047 Press, W. H., Teukolsky, S. A., Vetterling, W. T., and Flannery, B. P.: Numerical Recipes 3rd Edition:
1048 The Art of Scientific Computing, Cambridge Printing Press, Cambridge, England, 1986.
1049 Press, W. H., Teukolsky, S. A., Vetterling, W. T., and Flannery, B. P.: Numerical recipes in C: the art of
1050 scientific computing, Cambridge University Press, London, 1992.

Rothman, L. S., Gordon, I. E., Babikov, Y., Barbe, A., Chris Benner, D., Bernath, P. F., Birk, M., Bizzocchi, L., Boudon, V., Brown, L. R., Campargue, A., Chance, K., Cohen, E. A., Coudert, L. H., Devi, V. M., Drouin, B. J., Fayt, A., Flaud, J. M., Gamache, R. R., Harrison, J. J., Hartmann, J. M., Hill, C., Hodges, J. T., Jacquemart, D., Jolly, A., Lamouroux, J., Le Roy, R. J., Li, G., Long, D. A., Lyulin, O. M., Mackie, C. J., Massie, S. T., Mikhailenko, S., Müller, H. S. P., Naumenko, O. V., Nikitin, A. V., Orphal, J., Perevalov, V., Perrin, A., Polovtseva, E. R., Richard, C., Smith, M. A. H., Starikova, E., Sung, K., Tashkun, S., Tennyson, J., Toon, G. C., Tyuterev, V. G., and Wagner, G.: The HITRAN2012 molecular spectroscopic database, Journal of Quantitative Spectroscopy and Radiative Transfer, 130, 4-50, 2013.

Ryter, S. W. and Choi, A. M. K.: Carbon monoxide in exhaled breath testing and therapeutics, J Breath Res, 7, 2013.

Satar, E., Berhanu, T. A., Brunner, D., Henne, S., and Leuenberger, M.: Continuous CO2/CH4/CO measurements (2012–2014) at Beromünster tall tower station in Switzerland, Biogeosciences, 13, 2623-2635, 2016.

Schibig, M. F., Steinbacher, M., Buchmann, B., van der Laan-Luijkx, I. T., van der Laan, S., Ranjan, S. and Leuenberger, M. C,: Comparison of continuous in situ CO2 observations at Jungfraujoch using two different measurement techniques, Atmospheric Measurement Techniques , 8, 57-68, 10.5194/amt-8-57-2015, 2015.

Severinghaus, J. P.: Studies of the terresterial O2 and carbon cycles in sand dune gases and in Biosphere Doctoral Ph.D., Columbia University, New York, USA, 1995.

Steig, E. J., Gkinis, V., Schauer, A. J., Schoenemann, S. W., Samek, K., Hoffnagle, J., Dennis, K. J., and Tan, S. M.: Calibrated high-precision ¹⁷O-excess measurements using cavity ring-down spectroscopy with laser-current-tuned cavity resonance, Atmos. Meas. Tech., 7, 2014.

Stephens, B. B., Bakwin, P. S., Tans, P. P., Teclaw, R. M., and Baumann, D. D.: Application of a differential fuel-cell analyzer for measuring atmospheric oxygen variations, J Atmos Ocean Tech, 24, 82-94, 2007.

Sturm, P., M. Leuenberger, F.L. Valentino, B. Lehmann, and B. Ihly, Measurements of CO_2, its stable isotopes, O_2/N_2, and ^{222}Rn at Bern, Switzerland, *Atmospheric Chemistry and Physics*, *6*, 1991-2004, 2006.

Tennyson, J., Bernath, P. F., Campargue, A., Császár, A. G., Daumont, L., Gamache, R. R., Hodges, J. T., Lisak, D., Naumenko, O. V., Rothman, L. S., Tran, H., Zobov, N. F., Buldyreva, J., Boone, C. D., De Vizia, M. D., Gianfrani, L., Hartmann, J.-M., McPheat, R., Weidmann, D., Murray, J., Ngo, N. H., and Polyansky, O. L.: Recommended isolated-line profile for representing high-resolution spectroscopic transitions (IUPAC Technical Report), 86, 1931–1943, 2014.

Tohjima, Y.: Method for measuring changes in the atmospheric O-2/N-2 ratio by a gas chromatograph equipped with a thermal conductivity detector, J Geophys Res-Atmos, 105, 14575-14584, 2000.

Tran, H., Turbet, M., Hanoufa, S., Landsheere, X., Chelin, P., Ma, Q., Hartmann, J.: The CO2–broadened H2O continuum in the 100–1500 cm-1 region: Measurements, predictions and empirical model, Journal of Quantitative Spectroscopy and Radiative Transfer, 230, 75-80, 2019.

Valentino, F. L., Leuenberger, M., Uglietti, C., and Sturm, P.: Measurements and trend analysis of O2, CO2 and δ13C of CO2 from the high altitude research station Junfgraujoch, Switzerland — A comparison with the observations from the remote site Puy de Dôme, France, Sci Total Environ, 391, 203-210, 2008.

Varghese, P. L. and Hanson, R. K.: Collisional narrowing effects on spectral line shapes measured at high resolution, Appl. Opt., 23, 2376-2385, 1984.

Wójtewicz, S., Cygan, A., Masłowski, P., Domysławska, J., Wcisło, P., Zaborowski, M., Lisak, D., Trawiński, R. S., and Ciuryło, R.: Spectral line-shapes of oxygen B-band transitions measured with cavity ring-down spectroscopy, Journal of Physics: Conference Series, 548, 012028, 2014.

1100 Wolf, P. G., Parthasarathy, G., Chen, J., O'Connor, H. M., Chia, N., Bharucha, A. E., and Gaskins, H. R.:
1101 Assessing the colonic microbiome, hydrogenogenic and hydrogenotrophic genes, transit and breath
1102 methane in constipation, Neurogastroent Motil, 29, 2017.
1103 Zellweger, C., Forrer, J., Hofer, P., Nyeki, S., Schwarzenbach, B., Weingartner, E., Ammann, M., and
1104 Baltensperger, U.: Partitioning of reactive nitrogen (NO_y) and dependence on
1105 meteorological conditions in the lower free troposphere, Atmos. Chem. Phys., 3, 779-796, 2003.

1106

Reply to Reviewer 1 comments

We would like to thank Reviewer 1 for his/her supportive and interesting comments. We provided here detailed explanations/comments/modification. For clarity, we kept the reviewer´s comments in red and our replies in Black colors.

General observations:

General comments

The paper entitled *High-precision atmospheric oxygen measurement comparisons between a newly built CRDS analyzer (Picarro G-2207) and existing measurement techniques* describes a Cavity Ring Down Spectrometer devoted to the determination of oxygen concentration in air and to the delta ^{18}O isotopic ratio measurement depending of the instrument mode. The performances of the instrument are tested in laboratory by comparing measurements of well-known samples with results obtained using other techniques (IRMS, paramagnetic technique, Licor instrument) on the same samples. In the field measurements and comparisons are also provided by the authors at the High Altitude Research Station Jungfraujoch and at the Beromünster tall tower. The paper is well-written and detailed. The paper is now much easier to read thanks to the new way the experimental description and the obtained results are presented. The performances reached by the CRDS instrument are at the state-of-the-art for optical methods. The paper is fully in the scope of AMTD and is well-suited for a publication in this journal but needs some significant corrections (see the comments below).

Main remarks:

Part of the work in Fleisher et al. 2015 to which the authors refer in lines 135-141 seems to not be published. If authors have a published reference corresponding to Fleisher et al. 2015 they can let the text as it is but if they are not able to give a published reference they have to remove the lines 135-141 as well as the lines 144-146 and the reference.

The cited work by Fleisher is not yet a published article but exist as a conference paper. For this reason, we have now excluded this citation and its associated sections.

At the end of this paragraph we added the following sentence:

“Ultimately, the usefulness of the spectral model is to be evaluated by the precision and stability of the O_2 measurements when compared with established techniques.”

The concentrations reported in Figures 8, 12, 13 have to be given in the same unit (per meg or better in ppm) to facilitate the comparison. For example in Figure 13 it will be better to plot the two layers (the paramagnetic and the CRDS measurements) on the same graph using the same units.

We used the units ppm and per meg to reflect the actual measured values by the specific analyzers as we believe it will be best to keep the reporting as closely connected as possible to what we directly measure, which is optical absorption. By reporting what we actually measure, our reported values also show most honestly whatever is missing from the picture, such as the dilution due to unmeasured

carbon dioxide. But for some sections, we have provided measurement values in the same unit for better comparison between different analyzers for example Figure 16 and Table 1.

Regarding the "specific comments":

P2, L33: The authors have to recall the definition of *per meg* unit.

We have now added this definition at lines 35-40 as follows:

Note that the variations in atmospheric O2 is expressed in units of per meg due to its small variations with respect to a large background and to account for dilution effects from CO2 or any other gas of relevant amount change, which is expressed as:

$$\delta\left(\frac{O_2}{N_2}\right)(per\ meg) = \left(\frac{(\frac{O_2}{N_2})_{sample}}{(\frac{O_2}{N_2})_{reference}} - 1\right).10^6 \qquad (1)$$

P2, L43:The authors have to recall the definition of *the oxidation ratio* and give some explanations.

Defined in lines 50-51 as:

"OR defined as the stoichiometric ratio of exchange during various process such as photosynthesis and respiration"

P4, L86: The authors have to specify the reference of the pressure gauge, the proportional valve and acquisition board allowing stabilizing the pressure at the level of 3×10^{-5}!

The pressure is stabilized such that the error signal of the pressure sensor is 3 x 10-5. In other words, the actual pressure is (likely) not stabilized to that level, due to noise/drift in the sensor itself.

P4, L91: The authors should give the typical ring-down time they have.

We have now provided this information and added a sentence: "For this instrument the empty cavity ring-down time constant is about 39 μs."

P5, L104: Give here the FSR value instead of p7.

We provided the numerical value 0.0206 cm-1 in Line 105 and remove it from p7.

P6, L125: The authors should cite the following reference: Tran et al., JQSRT (2019) 222-223, p108- 114.

This reference is added Tran et al. 2019

Tran, H., M. Turbet, S. Hanoufa, X. Landsheere, P. Chelin, Q. Ma, and J.-M. Hartmann, 2019: The CO2-broadened H2O continuum in the 100-1500 cm-1 region. Measurements, predictions and empirical model. J. Quant. Spectrosc. Radiat. Transfer, 230, 75-80, doi:10.1016/j.jqsrt.2019.03.016.

P6, L142-144: This sentence is strangely written and should be reformulated.

As the reference to Fleisher and the discussion that goes with it are excluded, this part is also removed.

P7, L146-149: The excess noise observed by the authors is probably due to the fact that shorter ring-downs have less data points available for the fit. This should give a noise level increased by a factor of τ^(-3/2) where τ corresponds to the RD time.

We have observed some excess noise on the ring-down time constants for the highest loss points at the peak of the Q13Q13 line that is greater than the expected tau^(-3/2) dependence, which might be caused by absorption that is not linear in optical power, but we cannot be certain of this explanation at present.

P7, L158: Put also on Figure 1 the residuals when a Voigt profile is used. Moreover, the residuals observed on this figure seem to be due to a frequency shift and not to the limitations of the Galatry model. In the description of the Galatry profile, the authors don't mention the collisional line-shift parameter. Is this parameter taken into account for the calibration procedure? What about line- mixing effect?

P7, L.158: We have now revised Figure 1 considering the reviewer comment as follows:

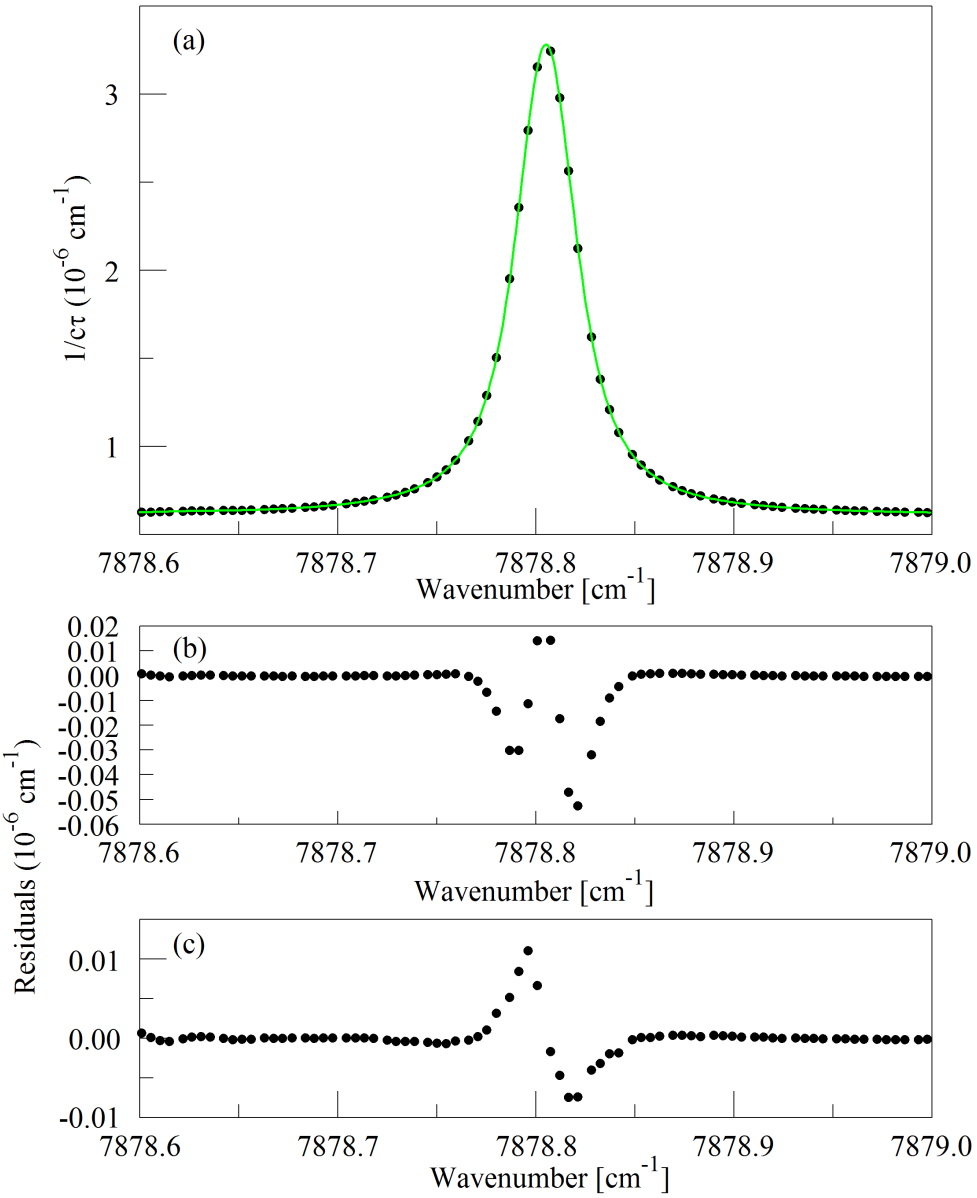

Figure 1. The top panel (a) shows the raw data (points) and the best-fit Galatry function (solid line). Residuals of the Voigt fit are shown in panel (b) and residuals of the Galatry fit are shown in panel (c).

Regarding the additional questions: (1) Yes, we take the collisional line shift into account in our calibration procedure, and (2) it is entirely possible that line mixing affects the line shape, but we are not in the position to say with confidence to what extent it does. This belongs in the class of line shape phenomena that we consider to be outside the scope of our measurement and modeling abilities, but which we also do not think are essential for the operation of the analyzer.

P7, L166: *frequency of narrowing collisions* should be replaced by *velocity change collision rate*.
This sentence is now modified accordingly

P7, L167: The authors should be more precise: …σ_D *is the* ***1/e*** *Doppler* ***half****-width of the transition*…

Corrected accordingly

P8, L169-170: The units of k_B, *T*, *M* and *c* have to be given.

The units of k_B, T, M and c are given as $J.K^{-1}$, K, amu and m/s, are now added to the manuscript

P8, L176: Cite HITRAN2016 instead of HITRAN2013.

We have now removed the citation of HITRA2013 and added HITRAN2016:

I.E. Gordon et al., The HITRAN2016 molecular spectroscopic database, Journal of Quantitative Spectroscopy & Radiative Transfer (2017), http://dx.doi.org/10.1016/j.jqsrt.2017.06.038 "

P8, L177: Give the uncertainty reported in HITRAN data base.
We have now added this information as "uncertainty code 4 for γ_{air} corresponding to 10% --20% relative uncertainty".

P8, L178: Change the reference if required (see my comment above).

Updated to HITRAN 2016

P10, L217-219: Not true for the line near 7878.45 cm^{-1} where the water transition dominates.

We would like to thank the reviewer for pointing out this important point. Indeed, we have not used the latest HITRAN2016 version water spectrum as this statement was derived from HITRAN2012. Hence:

- We added revised Figure 5, with a "stick plot" from Hitran2016 instead of Hitran2012.

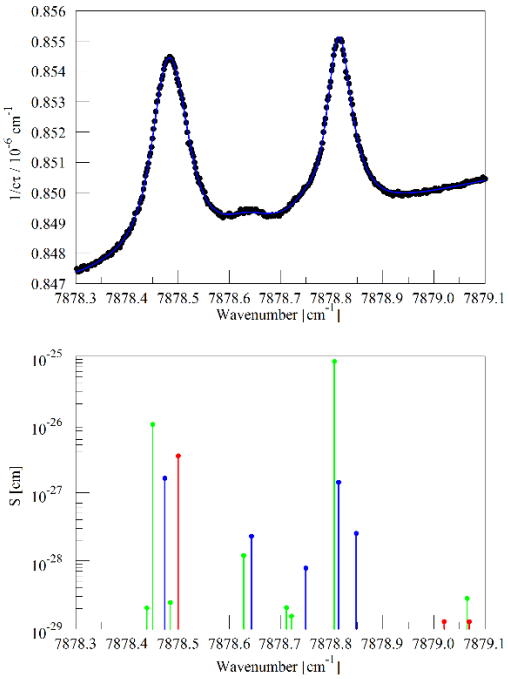

Figure 5. Upper panel: spectrum of water in nitrogen (points) and fit to Voigt model (blue curve). Lower panel: Oxygen (green), normal water (blue), and deuterated water (red) lines in the 2016 Hitran data base."

- We also replaced the sentence that spans lines 217-219 as "The main features are the Q13Q13 line from trace contamination of oxygen in the sample and several lines that arise from normal water ($^1H_2{}^{16}O$, AFGL abbreviation 161) and deuterated water ($^1H^2H^{16}O$, AFGL abbreviation 162, also abbreviated HDO)."

P10, L219-220: Three lines of HDO are missing in the figure but are present in HITRAN2016.

This is now corrected in the new figure 5.

P10, L222-L224: This is not true as HDO lines are present.

This sentence is also now rewritten as: "The relative intensities of the 161 and 162 lines change with variations in the isotopic composition of the water, but fortunately the direct interference with the oxygen Q13Q13 lines comes entirely from the 161 isotopologue, with the strongest 162 line being separated by approximately 8 line widths (FWHM) from the Q13Q13 line."

P11, L245: *the z-parameter was constrained to be proportional to y, based on earlier measurements.* This is not clear for me. What are these earlier measurements and how they show that? Same remark for line 250.

We have now changed the words "earlier measurements" on line 245 to "measurements summarized in Figure 2". This figure shows that to a good approximation y and z are both proportional to pressure and therefore to each other when the pressure changes.

P11, L251-253: How the missing HDO lines will be treated as the HDO isotopic abundance is not determined from the 7817 cm^{-1} window.

P11, L251-253: The text describes what we did. To address this we now added a sentence between the sentence that ends on line 253 and the sentence that begins on line 254 as follows: "This procedure does not account for variations in HDO abundance, which may introduce some systematic error into the water vapor correction for samples of unusual isotopic composition, but it should accurately model the most important lines that interfere with the oxygen measurement."

P12, L277: *sccm* instead of *scm*.

Corrected accordingly

P13, L299-308: Maybe adding equations will make this paragraph easier to understand.
As there are in-line equations that clearly explain that by using the ratio of amplitude to line width rather than amplitude alone we obtain better precision in the determination of O_2 concentration, we do not see the importance of adding additional equations at this section.

P14, L326-329: What about the water lines in that spectral region (especially the H_2O line near 7881.98 cm^{-1})?

We are aware of these lines; they do not interfere strongly, as they are about two full-widths away from the line we measure.

P19, L436: It is strange that only the last one minute of data was considered to determine the concentration for each standard by CRDS as each standard was flushed during 2 hours before.
Selection of the last one-minute data done to be consistent with ambient air measurements which are usually switching from one height level to another and between standard cylinders usually within a couple of minutes.

P20, L464: *DAS* has to be defined.
We have now replaced the acronym DAS with "temperature inside the instrument chassis" as DAS seems to be too technical.

P20, L474-478: It would be very interesting to know the origin of the problem and how the manufacturer solved it. As people from *Picarro* are co-authors of this paper it should be easy to have such information's.
We have now included a possible hypothesis that could have led to such a drift to this line as follows:

"A possible hypothesis for the cause of the drift can be an optical amplifier in the first system and not anymore included in the design of the product which produced a significant amount of broadband light that could fill the cavity (albeit with a low coupling coefficient), and would ring down with a different (and generally much faster) time constant that the baseline loss of the cavity. However, the ringdown time on the peak of the oxygen line is just 10 microseconds, such that the broadband light might have distorted the single exponential decay of the central laser frequency, leading to the observed drift in the oxygen signal. However, we were not able to confirm this hypothesis."

P27, L631: *An excellent agreement was observed for measurements from both instruments…* Not so easy to check on Figure 18 (see the comment below).

P27, L634: …*contains large amount of water* ***and*** *CO_2 in addition to O_2*…

Corrected as mentioned above

Figure 5, lower panel: Add the missing HDO lines (see HITRAN2016). For example the transition $4_{1\,3}$- $3_{1\,2}$ of the 111-000 band near 7878.500 cm^{-1} has an intensity of 3.47×10^{-27} cm/molecule.
We have now modified Figure 5 as explained above

Figure 14: What is the scale on the left?
It is mmol/mol but uncalibrated values and now added to the Figure as shown below

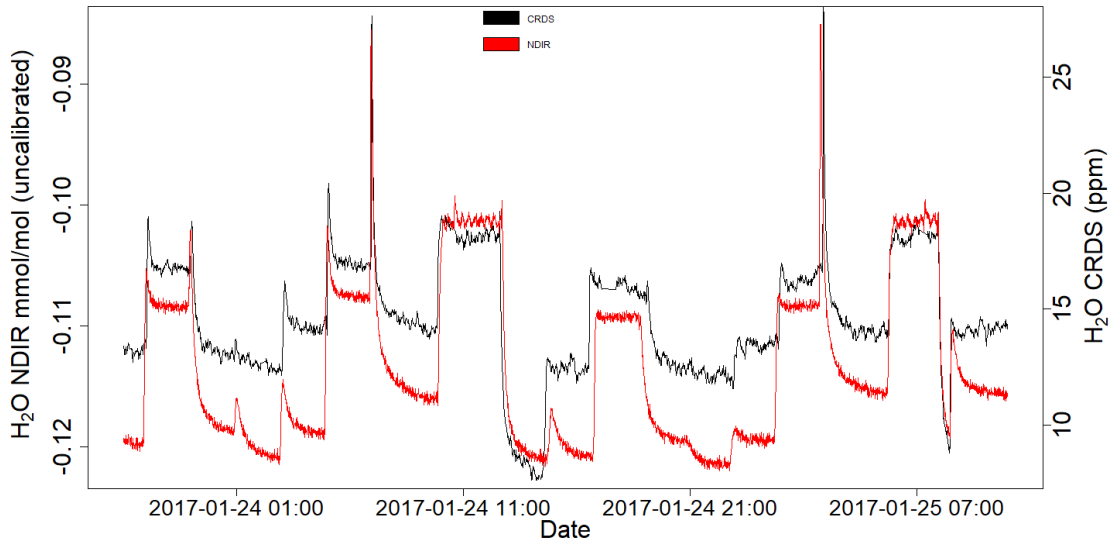

Figure 14. Parallel water vapor measurements for a dried ambient air by both the NDIR and CRDS analyzers. Note that the water values from the NDIR analyzer are not calibrated.

Figure 18: The peaks corresponding to the flasks are not observed at the same time for the CRDS and IRMS. Moreover the delay between both experiments varies from one peak to the other. What is the reason for that? It will be better for comparison purposes to plot the two layers on the same graph.

This difference is simply due to the difference in time stamps from the two analyzers and the two are not plotted in the same figure as the purpose here is to provide a quantitative view of the peak signs. We have now added the time stamps for both plots in the x-axis (figure below).

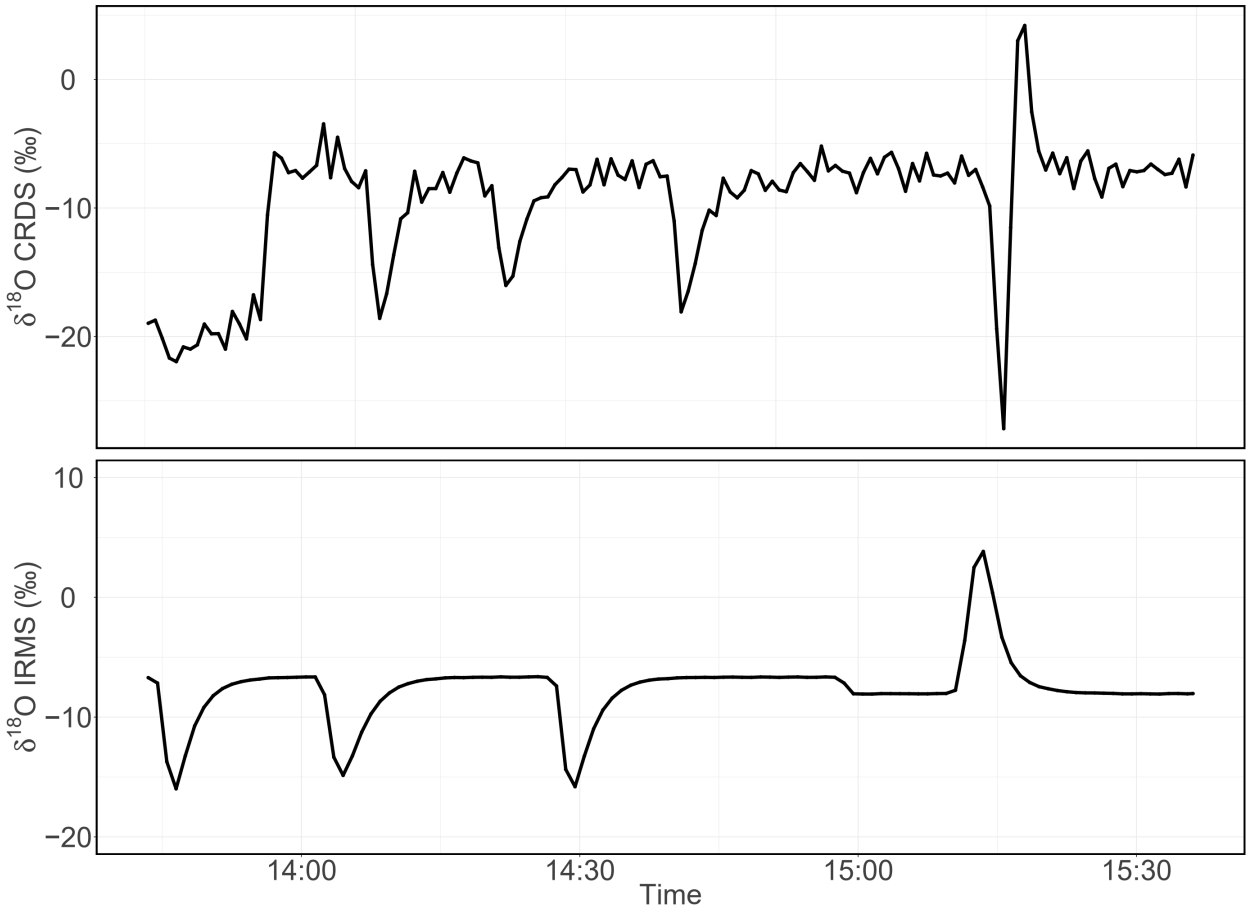

Figure 18. Consecutive $\delta^{18}O$ measurements of a standard gas (CO_2-free air) filled into three flasks followed by measurement of breath air using the CRDS analyzer (top) and IRMS (bottom). These measurements were carried out in the middle of ambient air measurements.

Reply to Reviewer 2 comments

We would like to thank Reviewer 2 for his/her supportive and interesting comments. Unfortunately, these comments were made based on the first version of the manuscript, after we made thorough reorganization after suggestions by the Editor. It also makes it difficult understanding where these comments are located but we tried all our best. We provided here detailed explanations/comments/modification. For clarity, we kept the reviewer´s comments in red and our replies in Black colors.

Review of manuscript "High-precision atmospheric oxygen measurement comparisons between a newly built CRDS analyzer (Picarro G-2207) and existing measurement techniques" by Tesfaye A. Berhanu et al. submitted to Atmospheric Measurement Techniques General comments:

This paper from A. Tesfaye et al. presents the principle, the method and experimental tests conducted on a new CRDS analyzer dedicated to high precision oxygen measurements in the atmosphere and possibly additional measurement of isotopic content of O2. The first in-situ monitoring results obtained with this instrument are also presented and compared to other current existing measurements technics running in parallel. In the introduction, the authors remind us about the scientific context and the scientific interest to measure O2 mixing ratio in the atmosphere, in the framework of carbon cycle budget and natural/anthropogenic source/sinks attributions, due to the strong link between the oxygen variability and the carbon cycle (combustion and respiration reactions). Then they highlight the analytical challenge to obtain a high precision measurement of O2 due to the very low level of atmospheric variability and they then shortly review the existing measuring technics currently avail- able and the main experimental difficulties associated. In the second section, (Materials and methods), part 2.1, there is a description and discussion of the analyser design principles and characterizations (p4-14). The authors first describe the general instrument principle and design (including associated program modules), then explain the best conditions to be met for an ideal high precision measurement of molecular oxygen and finally constrains linked with an operational deployable field instrument. This provides them justification for the technical and methodological choices made such as spectroscopic model used, water vapour measurement and correction considerations, O2 measurement method design as well as O2 isotopic content measurement. On my opinion this section is a bit too long (about 1/3 of the full article) and also sometime a bit difficult to follow as a non-specialist of spectroscopy. I would suggest to shorten and simplify a bit this section if possible so that it can be more easy to follow. In the case it is not possible to shorten it I would recommend to modify the title of the article to better take into account this section which is anyway useful and interesting (but at the moment reading the title, I would expect the work to focus more on instrumental atmospheric data inter-comparison than technical and spectral analysis).

We are aware that the spectroscopy section comprises significant part in this manuscript. However, we would like to keep these sections in the manuscript in line with Reviewer 1, who requested as much detail as possible about spectroscopy. We understood the need for reflecting this in the title of the manuscript but our main focus is still the intercomparison study between these analyzers.

The second subsection (part 2.2 and following) presents the instrumental tests and evaluation conducted in the laboratory at Picarro, at the University of Bern and in the field in Switzerland (two sites, Jungfraujoch and Beromünster). Experimental set up and conditions as well as methodologies adopted for the tests are presented in these subsections. The last section (section 3) presents and

discuss the results of the different laboratory tests and in-situ monitoring. I would suggest to re-organize a bit this section with the previous one. I think this would be easier for the reader to follow if the test results (in section3) were merged together with the description of the tests procedure (in section 2). So I would merge 2.2.1 with 3.1.1, 3.2.2 with 3.1.2 (actually labelled 3.2 but should be 3.2.2) and also 2.3.3 and 3.2.3 (water correction). I would then keep all the in-situ parts together in section 3.

We believe there is a small misunderstanding to which version of the manuscript these comments are provided. While we submitted our manuscript for the first time indeed we have these sections separated. But based on the recommendations of the Editor we have modified these sections similar to the comments given above. For example section 2.2.1 does not exist in the final version of the manuscript published here but rather merged to section 3.

In the last subsection, the authors present some results for test conducted with the analyser on the isotopic mode. The paper ends with a last concluding section. 2 One general comment and concern of this paper is the reporting unit used for O2 concentration all over the article. The authors used either the ppm unit (most of the time) or the per meg unit (also depending on the instrument used). As there are inter-comparison results used here to validate the new instrument but presented with a mix unit data, it is not easy to follow and to fully compare all data sets as well as precision of the different methods and instruments. Even though there is currently no official international unit to report O2/N2 mixing ratio, and also no Central Calibration Laboratory, there were recommendations given in the last WMO GAW report (report n□242) to report the O2/N2 mixing ratio in per meg units and also if possible to report it on the Scripps Institution of Oceanography (SIO). I would then suggest to make a choice of unit (preferentially per meg) all over the paper and present all the results in a uniform way. When necessary there is a relationship that might be used to express changes in O2/N2 ratio and equivalent changes in O2 mole fraction (Keeling et al, 1998; WMO GAW report n□ 142). Having all number on the same unit would greatly help in the data comparison sections and table 1 (for example) except if this is not applicable. My general feeling about the paper is good, it is generally well written and most of the time clear. I would recommend this article for publication in AMT after revision, as this is a quite interesting new method to measure O2 with a great potential for atmospheric monitoring. Nevertheless, I would highly recommend to take into account the remarks and suggestions raised in the present review in order to straighten and improve the present manuscript. In particular, some additional calculation of mean values and standard deviations would help better evaluate the performances of the instrument compared to current ones.

We used the units ppm and per meg to reflect the actual measured values by the specific analyzers as we believe it will be best to keep the reporting as closely connected as possible to what we directly measure, which is optical absorption. By reporting what we actually measure, our reported values also show most honestly whatever is missing from the picture, such as the dilution due to unmeasured carbon dioxide.

In times where conversion is needed for comparison purpose, we provided the measurements from different analyzers in ppm unit for example Figures 15 &16.

Regarding Table 1, as it is clearly shown, we have provided all the oxygen values in per meg units and CO2 values in ppm.

Specific comments:

Abstract

Line 21: May need to precise that the given short term precision given here refers to the O2 mixing ratio (not to the isotopic ratio).

We have now specified this by modifying this sentence as "…standard error of one-minute O_2 mixing ratio measurements …."

Line 21-23: In this sentence the authors state that the long term stability of the instrument is excellent and prevent high frequency calibration to assess an overall uncertainty of <5 ppm. The recommended calibration frequency is every 12h. With regards to my knowledge and own experience, paramagnetic technics only recall 24h calibration frequency to achieve similar precision. So I would suggest to moderate a bit this sentence, especially the beginning "In contrast to the currently existing techniques".

This statement is partly correct. Indeed, a full calibration for the paramagnetic technique is also made every 18 hour but a frequent 18 minute offset correction is applied since the drift rate of a paramagnetic cell is immense despite a thorough control of the pressure and temperature. In our sentence we refer in particular to the short-term drift that is much better than for corresponding techniques and therefore, we would like to keep this sentence as it is.

The section two of the paper "material and methods" which is the longest part of the paper is not really mentioned in the abstract. May be a few more words should be added in the abstract to remind the reader about the work described in this later section.

We have now added a line to reflect this point in the abstract as follows:

"Here we present detailed description of the analyzer and its operating principles as well as comprehensive laboratory and field studies for a newly developed high-precision oxygen mixing ratio and isotopic composition analyzer (Picarro G-2207) that is based on cavity ring-down spectroscopy (CRDS)".

Introduction:

The introduction section is not labelled as for the other sections (it should be section 1).

It is now labelled as section 1

Line 34-36: I would suggest to update the CO2 mixing ratio to the one of year 2017 (around 405 ppm).

Modified to 405.0 ppm

Line 47-51: There are also WMO/GAW precision recommendations and guidelines for O2/N2 ratio, as describe in the last GAW report (GAW report n ◦ 242, table 1 and p42-44).

We have now added this information on Line 70 as:

Note that the GAW recommendation for the measurement precision of O_2/N_2 is 2 per meg.

Line 55 and 56: Gas chromatography => gas chromatography

Corrected as suggested

Lien 57: As far as I know the techniques described in the previous sentence are not really commercially available. The sensors or detectors can be delivered by commercial companies but cannot be used directly to monitor O2 concentration. There is a need to "customize" these 3 detectors to build a monitoring instrument reaching the precision goal needed for atmospheric monitoring. This is most of the time done by the laboratories themselves!

We agree with the reviewer here. Instruments capable of making O2 measurements of the well-mixed atmosphere at anything close to the precision needed for the scientific goals of the atmospheric community are neither commercially available nor widely used. These are custom-built analyzers that require a great deal of expertise to set up and run them, and to interpret the results properly.

We have removed part of the sentence "commercially available" and the beginning of this paragraph now reads as:

"Currently there are several techniques mostly custom built that can measure…."

Line 61: I would add the following words at the end of the sentence: ". . . of the analysis method especially for continuous monitoring".

We have now added "…especially for continuous monitoring" to this section.

Material and methods:

Analyser design principles:

Line 79: Please define DFB

DFB signifies Distributed Feedback and this term used now in the manuscript instead of DFB.

Line 99-100: What is the typical range of variation for noise between the different instruments?

As far as noise-equivalent absorption goes, that varies by as much as a factor of two between instruments.

Line 102: This is the first time that the Per meg unit it used in the paper (i.e. ppm is used most of the time). As already stated, it would be better to choose and harmonized the unit all over the paper.

We have now defined the per meg unit with equation as follows in the manuscript:

Note that the variations in atmospheric O2 is expressed in units of per meg due to its small variations with respect to a large background and to account for dilution effects from CO2 or any other gas of relevant amount change, which is expressed as:

$$\delta\left(\frac{O_2}{N_2}\right)(per\ meg) = \left(\frac{(\frac{O_2}{N_2})_{sample}}{(\frac{O_2}{N_2})_{reference}} - 1\right).10^6 \qquad (1)$$

Line 116: I'm not an expert in spectroscopy, and the formalism used here to describe the absorption band is a bit unclear for me and a non-specialist. I don't know if there is a way of clarifying or simplifying this another way?

We provided the details of transitions we measure with the quantum numbers of the states measured. However, the main concept here, for a non-spectroscopist, is that we measure a single, isolated absorption line in the 1.27 micron band.

Line 143-145: This sentence is not clear, I suppose there is a verb missing: "In addition, the optical power in the ringdown cavity IS set by the ring-down detector threshold, which . . ."

This section is now excluded from the manuscript as suggested by Reviewer 1

Line 159-160: This sentence is not clear: I think it should be "It stands out that the residuals that are largely an odd. . ."

We clarified this sentence as:

"It stands out that the residuals are largely odd in detuning from the line center…"

Line 185: Can the authors argue why they consider the dependence of Z on O2 too small to be significant?

The measurements show that any variation is at most comparable to the error bars, so we do not consider it a significant effect.

Line 196: please correct "for in measurements".

The word "in" is now removed

Line 224: Can the author explicit what they mean by 161 isotopologue of water. This is absolutely not clear for a non-specialist in spectroscopy.

This sentence is now modified as follows:

The main features are the Q13Q13 line from trace contamination of oxygen in the sample and several lines that arise from normal water ($^{1}H_{2}^{16}O$, AFGL abbreviation 161) and deuterated water ($^{1}H^{2}H^{16}O$, AFGL abbreviation 162, also abbreviated HDO).

Line 277: Please define "scm".

It is now corrected as "sccm" meaning Standard Cubic Centimeter per Minute

Line 300: I would suggest to change ". . . adds additional .." to ". . . adds more. . ."

Now modified accordingly

Line 308-309: I'm a bit surprised that the instrument is providing a dry mole fraction for O2 using the water dilution experiment as it is stated by the authors above in the manuscript (line 273-274) "more works need to be done to investigate the water vapour correction of the oxygen measurement". My feeling is that the present day correction is still not fully satisfying and should be used with caution! There is also no direct explicit correction equation given in the text nor explanation on how this correction is implemented (or to they use the directly the linear function given on figure 7?).

Complete validation of the water vapor correction has not yet been performed, and is beyond the scope of this paper.

As for the numerical details, the linear fit in Figure 7 determines a linear relationship between optical absorption and water fraction, and the correction to oxygen is just the usual dilution correction.

Line 327-330: Taking into account the low precision of the analyser for isotopic content as stated by the authors, is there still an interest to measure them within the context of environmental studies? Could the authors give us a few example and/or possible application of O2 isotope measurement in the environment that could be achieve with that instrument?

We are not quite sure whether we understood the reviewer's comment correctly. Therefore, we refer to the two issues we can think of. First, regarding the degraded precision of the concentration measurement in the isotope mode. This is due to choosing a weaker main oxygen line to be closer to the minor isotope line selected and a significantly reduced number of ring-downs for the main oxygen line to favor the precision of the minor isotope line. Here, a further optimization depending on the users' needs is possible. Secondly, the interference on the isotope ratio itself on breath air is not yet understood. Further measurements are required to see which substance or substances are responsible for this interference. We would like to mention, though, that measurements on the compressed air composition led to a good agreement. Therefore, we can think of the following applications in the field of environmental research. Biological applications relevant for the climate and environmental research, i.e. photosynthesis/respiration processes close to the plants or even using leaf chambers. Analysis of vertical profile air samples taken by means of an AirCore is another application. First measurements have been taken in 2018. Here, stratospheric-tropospheric differences can be a focus. Many other process studies can be thought of where the oxygen is involved, e.g. combustion processes, electrolysis where incompleteness of the process will lead to isotope anomalies.

Another important application is in isotopic tracer experiments, in which either isotopically labeled carbon dioxide or water can be introduced into a closed plant system to understand better the photosynthesis. The isotope labeling can be performed at levels where the signals are greater than the errors in the measurement.

Laboratory tests at Picarro, Santa Clara:

This section and following subsections should be relabelled, 2.2; 2.2.1; 2.2.2 etc. . .

These sections have been modified and merged to section 3 of the manuscript as suggested by the Editor

Line 346: Please define sccm.

Defined above

Laboratory measurements at the University of Bern:

Line 351-355: Could you please add a reference describing the Bern O2 analytic measurement systems (Both for The Fuel cell system and for the Mass Spectrometer) if available.

We have now added the following reference:

Sturm, P., M. Leuenberger, F.L. Valentino, B. Lehmann, and B. Ihly, Measurements of CO_2, its stable isotopes, O_2/N_2, and ^{222}Rn at Bern, Switzerland, *Atmospheric Chemistry and Physics*, *6*, 1991-2004, 2006.

Line 356: Could you please give us a bit more details about the "pressure controlling unit": What is it, What kind of flow meter? (short description or reference).

The pressure control system includes an electronic controller (Type 250E, MKS) which maintains a pressure difference of zero (precise to 0.005 mbar) across the pressure transducer (Baratron 223, MKS) by adjusting the waste flow using the nearby solenoid control valve (Type 248, MKS)

Line 367-377: I'm a bit surprised that there was no direct measurement made to the IRMS without the tee junction. To my knowledge the IRMS is the only one instrument that can provide a very high precision O2/N2 measurement and should be seen as the reference instrument. So I would have made the test in three steps, first with the Tee measuring on both instruments, then directly on the IRMS without the tee which would have given a reference value and then directly to the Picarro. All this at the different splitting ratios. Is there a reason why the direct measurement to the IRMS was not done?

Actually, there is no specific reason why a direct measurement was not conducted on the IRMS. However, as we conducted comparison of the CRDS analyzer and the IRMS by directly measuring multiple standard gases (See Table 1), we believe it can provide an excellent estimate of how the CRDS measurements are comparable to the IRMS.

Line 380: please replace "case b" by "case ii".

Corrected to Case ii

Line 378-389: The conclusion of this section are a bit disappointing as none of the results are shown and only one value is given (without uncertainty). Would it be possible to show the results of the tests? Previous studies by A. Manning have shown that the tee junction effect could be relevant at the level of precision that we are looking for atmospheric O2 monitoring. The impact given here (0.5ppm) is already more than half of the global precision stated for the instrument (<1 ppm line 23). So, if the instrument is to be commercialized, I would deeply recommend to go deeper into that question and firmly establish the conditions of use of a Tee junction or not.

We agree with the reviewer that it is important to further investigate the tee junction influence on the O2 measurements. During this test period, we have tried to test different scenarios of splitting ratios effect. Unfortunately, our observations are inconclusive which is mostly attributed to the temperature effect observed while decanting a cylinder at high flow. Note that the CRDS analyzer takes about 45ml/min and if we would like to go for a splitting ratio of 1:100, we need to decant the cylinder at a flow of 4.5 L/min, which led to cooling effect at the cylinder gauge. As A. Manning has also shown that temperature plays a major role in fractionating oxygen. Meanwhile, the analyser is commercially available and we ask users to make their own tests or use split ratios if needed in the range where we document the values in the manuscript.

Line 403: How was established this correction function? What is the link with the test from figure 7? See also comment for line 308-309.

Already replied above

Line 424: Add a reference to JFJ measurements and set up.

We have now added the requested reference:

Schibig, M. F., Steinbacher, M., Buchmann, B., van der Laan-Luijkx, I. T., van der Laan, S., Ranjan, S. and Leuenberger, M. C,: Comparison of continuous in situ CO2 observations at Jungfraujoch using two different measurement techniques, Atmospheric Measurement Techniques , 8, 57-68, 10.5194/amt-8-57-2015, 2015.

Line 465: Please remove "is avoided" at the end of the sentence. Can the authors give us more precision about what they call "preconditioned"?

The word "is avoided" is now removed

Preconditioning is a standard procedure at our lab for all flask samples prior to using them for sampling. A dedicated vacuum line was used to pump these flasks to vacuum, then flush multiple times with dry air and fill them to 1 atm with this air prior to sampling.

Line 463-469: I have one question regarding this evaluation. Why do the authors use glass flasks? Why not connecting directly the CO2 free cylinder to the analytical device? This would avoid potential contamination during flask filling.

Its simply because it is easier to for experimental set up for example as we were placing these flasks before and after a water trap, which cannot be easily done with the cylinder.

Results and Discussions: See general comments for re-organisation proposition.

As we mentioned in the sections above, these comments were made on the first version of the MS and these reorganizations have already been applied.

Line 483-490: Looking at figure 9, it doesn't seem to me that there is a real drift. For me a drift would show a smooth continuous tendency to increase or decrease in the values. Here what I see is more something like a large variability on the measurement, I see an anti-correlation between O2 values et Y parameter and to a lesser degree a correlation between peak height and O2 as well. So I don't really understand what the authors mean by drift here. Could you please clarify. Are there also some ideas to eliminate or identify those small drift as stated on line 490?

It should be noted here that the measurement that the instrument reports is not Gaussian in nature, such that the Allan std. deviation does not decrease according to the square root of averaging time for long times (> 1 hour).

To clarify more this paragraph and in agreement with the reviewer's comment, we have now replaced the word 'drift' with 'error' as "the residual error of the analyzer…." And "Possible sources of error…..".

Line 511: What is a very good agreement? Can the authors give us an estimate of the mean difference (on a comparable unit for example?). This would help to evaluate the accuracy of the

new instrument and see how well it meets the WMO recommendation or not. Same goes for table 1 which is difficult to use because of the different units for the different instruments!

We intentionally converted the O2-CRDS values from ppm to per meg units to make them comparable. As can be seen from table 1 the three Scripps cylinders (ST3-ST5) IRMS UBern measurements are in agreement with the assigned values by Scripps to 0.6 ± 3.7 per meg, the O2-CRDS measurements for those 5.6 ± 17.8 per meg and the O2-Parameagnetic measurements show a comparison of 20.6 ± 26.8 per meg. A similar agreement is obtained between the three methods when including the cylinders ST-1 and ST-2 prepared by UBern. The picture is different for the ST-6 and ST-7 for known reasons as explained in the manuscript.

Line 517-519: This is absolutely needed if the final goal is to get high precision O2 measurement. There is no need for high precision CO2 measurement but this dilution effect is to be taken into account as already done with present day "homemade" monitoring systems, even for atmospheric monitoring purpose.

Here we are referring to a cylinder with 2700 ppm CO2! As we mentioned in multiple sentences including the conclusion section, it will be important to have a parallel CO2 measurement (or the possibility to have a second laser for CO2, at least in the future) to account for dilution effect. As a side note any kind of gas addition to an ambient air will lead to a gas dilution effect. This even includes using compressed air by gas filling company or self-made ambient air compression when there small leak in the compression line, which could alter the gas mixture. Which could, for instance, lead a change in Ar/N2 or O2/N2. Even more care should be taken when using artificially compressed air-like gas mixtures. Here a proper determination of the gas components needs to be done.

Line 521: Please change "The measurement precision of the Picarro G-2207 measurement was calculated. . ." to "The measurement precision of the Picarro G-2207 measurement was calculated. ."

This comment is not clear. But we changed the text as:

"The measurement precision of the CRDS analyzer was calculated. . ."

Line 521-526: What about the precision of the reference instrument that should be the IRMS?

See answer to the question above (line 511…)

Line 527- 536: I fully agree that it is difficult to compare the graph as there is this problem of unit already highlighted in this review. I'm not sure how significant is the small difference in the correlation coefficient calculated here.

The fact that the mean offset as well as the standard deviation of the measurements of ST-1 to ST5, as given above in the answer to question line 511…., is larger for the paramagnetic cell (at least for the instrument at UBern) than for the CRDS instrument, can easily clarify our statement in this line.

Line 541-542: I agree that the drift at the beginning could be linked with unstable condition after unpacking but the drift remains all over the measuring period and usually Picarro are stable within 3-5 hours after starting measurements. Line 551-553: Did the manufacturer find the cause of this drift. Was there any significant change in the hardware or software configuration of the initial instrument?

One possibility for the cause in the drift was an optical amplifier in the system, which produced a significant amount of broadband light. This light could fill the cavity (albeit with a low coupling coefficient), and would ring down with a different (and generally much faster) time constant that the baseline loss of the cavity. However, the ringdown time on the peak of the oxygen line is just 10 microseconds, such that the broadband light might have distorted the single exponential decay of the central laser frequency, leading to the observed drift in the oxygen signal. We were however not able to confirm this hypothesis. There is no optical amplifier in the present design of the product.

Line 558-562: Did the authors also made water measurement comparisons between Licor and Picaro on wet air conditions?

We have made all the LICOR measurements using wet samples. However, we did not make an absolute comparison between the LICOR and CRDS analyzers for two reasons:

- First the LICOR water measurements are not calibrated (it of course could be done but firstly this would be outside of the scope of this publication and secondly we generally dry the ambient air)

- Second our focus in this manuscript was not comparing the water measurements by both devices

But as it can be seen in Figure 14, the water measurements from both analyzers for dried and non-dried air show similar behavior with matching water peaks

Line 564-565: This sentence is very confusing. Please reword as follow: ". . . in O2 measurements in both cases. (Figures 15c & 15d) shows in case. . ."

This section is now rephrased as follows:

"The water correction test was conducted by measuring dried ambient air (Figure 15a) into both analyzers as well as allowing non-dried air to the CRDS analyzer only (Figure 15b) and comparing the difference in O_2 measurements in both cases. Figures 15c & 15d show the water contents of dried ambient air measured in both analyzers (note that the CRDS uses its in-built water correction function)."

Line 573-577: Can the authors provide some more precise numbers such as for example mean values and standard deviation calculated from data shown in figure 15c and 15d. This would greatly help quantify the variability and give a comparison element with regards to the given instrumental precision.

For 15 c, mean = 1.85, Standard deviation=6.8

For 15 d, mean = -10.4, Standard deviation=14.6

Line 581-583: I disagree with this statement, there are several sections of the paper dealing with the water correction factor. There was a choice stated in the paper and made by the manufacturer to enable wet air measurement, so the water correction is a key issue if the instrument is going to be sold soon and to assess high precision measurement. I'm convinced the correction factor is not easy task to handle and the results presented here are not sufficient to close the problem and give a final solution but this has to be further investigated.

We fully agree with the reviewer that further and even more detailed and extended water correction analyses have to be performed, but we do not agree that it should be part of this publication. We note that for the most of the instruments on the market further improvement of correction functions are found over time. This will certainly also be the case here.

Line 585-593: How are the Picarro data calibrated (based on the in-situ calibration cylinders that have been measured also I suppose)? Could the author quantify a bit more precisely the "very good agreement" like for example providing the mean and the standard deviation of the data for both analysers over the full period. For me, based on the figure 16, it seems that there is a little offset between both instrument (paramagnetic a bit lower) and that there is a slight higher variability for the Picarro instrument compared to the other one but it is difficult to assess with only the figure.

Yes, the Picarro data is calibrated using the standard cylinders measured in-situ.

This question is a bit unclear. These are ambient air measurements with natural variability (on top of the variability from the analyzers) and we do not see the point of providing the mean and sd of these measurements.

If what the reviewer is implying here is for the difference, the calculated mean is -0.33 ppm and a standard error of 0.11 ppm.

Line 595-607: I understand that the isotopic mode is not well suited for ambient O2 concentration measurement but what about the isotopic values? Any comment about those?

Yes, this in an interesting question. The isotope values of ambient air after calibration using internal standards corresponds to expectations. The short-term (second) variations are large but the standard deviations of 5 minute means corresponds to about 0.3 permil.

Line 641: Can the authors provide a table with the individual values for each flasks and instrument so that we can really compare the results and evaluate the precision and repeatability of the measurements on each instrument? Can we add mean values and standard deviation for the three replicates?

We do not think it is relevant to include these values in the manuscript as we already stated that the isotope measurements from the CRDS analyzer needs a closer look but the plots in Figure 18 already gives a clear idea about the above mentioned topics.

Line 644: I think the authors mean ". . .of water and CO2 in addition. . ."

Corrected accordingly

Line 653-655: Would the authors then recommend using the isotopic mode of the instrument at the moment (at least for atmospheric monitoring on atmospheric range) or still need some work to improve it and be sure it is reliable? (at least for atmospheric monitoring on atmospheric range)?

This analyzer cannot measure natural isotopic variations. But, it can be used in tracer experiments where artificially enriched isotopes are used to study various biological processes such as photosynthesis. However, the manufacturer will continue to work on improving it.

Conclusion:

Line 672-677: I feel that the conclusion driven here are a bit optimistic. It is stated several time in the paper that there is still work to do on this question. I would suggest to reword a little bit that conclusion in that way.

We have now added the following sentence recommending for further tests about the water correction.

"However, we believe that it is important to further investigate this issue and identify an improved water correction strategy."

Line 680-681: Here also I would like to see the data with mean values and standard deviation before drawing such an optimistic conclusion (see comments in the previous sections). I think this conclusion also lack a more general statement about the future applications of this instrument and possible improvement (especially for the isotopic mode).

We have now added the following sentence at the end of this paragraph:

"However, we believe that this analyzer can be used for tracer experiments where artificially enriched isotopes are used to study biological processes such as photosynthesis in plants using isotopically labelled CO_2 and H_2O".

Figure 1: The parameter τ is not define neither in the legend of the figure nor in the text. I wonder why the measurements presented here are made at 333Hpa and not at 340 hPa which is the nominal working pressure of the instrument (see line 86)

Tau is just the averaging time for the Allan variance. All measurements with this analyzer were made at 255 Torr, which are same as 340 hPa.

Figure 9: There are strange value above each of the three upper graphs (+2.1028e5 on the upper one). What do they mean?

This is a notation to indicate an offset of the y-axis. In other words, the oxygen fraction reported in the top panel of what is now Figure 8 varies by about 12 ppm about a value of 2.1028e-5.

Line 773: correct "shown to show".

Corrected as "show"